Supporting information for

Tricarabrols A-C, three anti-inflammatory sesquiterpene lactone trimers featuring methylene-tethered linkage from *Carpesium farberi*

Jie Yuan, [‡, a, b] Xuelan Wen, [‡, c] Chang-Qiang Ke, [a] Tian Zhang, [d] Ligen Lin, [d] Sheng Yao, [a] Jason D. Goodpaster, [c, *] Chunping Tang, [a, *] Yang Ye [a, e, *]

[a] State Key Laboratory of Drug Research, and Natural Products Chemistry Department, Shanghai Institute of Materia Medica, Chinese Academy of Sciences, Shanghai 201203, China

[b] University of Chinese Academy of Sciences, No. 19A Yuquan Road, Beijing 100049, China

[c] Department of Chemistry, University of Minnesota, Twin Cities, Minneapolis, Minnesota 55455, United States

[d] State Key Laboratory of Quality Research in Chinese Medicine, Institute of Chinese Medical Sciences, University of Macau, Taipa, Macau, China

[e] School of Life Science and Technology, ShanghaiTech University, Shanghai 201210, China

Table of Content

Figure S1. IR spectrum of compound **1** 4
Figure S2. HRESIMS spectrum of compound **1** 4
Figure S3. ECD spectrum of compound **1** 5
Figure S4. ^{1}H NMR spectrum of compound **1** in $CDCl_3$ 5
Figure S5. ^{13}C NMR and DEPT spectrum of compound **1** in $CDCl_3$ 6
Figure S6. HSQC spectrum of compound **1** in $CDCl_3$ 6
Figure S7. HMBC spectrum of compound **1** in $CDCl_3$ 7
Figure S8. ^{1}H-^{1}H COSY spectrum of compound **1** in $CDCl_3$ 7
Figure S9. ROESY spectrum of compound **1** in $CDCl_3$ 8
Figure S10. Selective HSQC (C15-30) spectrum of compound **1** in $CDCl_3$ 8
Figure S11. Selective HSQC (C30-45) spectrum of compound **1** in $CDCl_3$ 9
Figure S12. Selective HMBC (C15-30) spectrum of compound **1** in $CDCl_3$ 9
Figure S13. Selective HMBC (C30-45) spectrum of compound **1** in $CDCl_3$ 10
Figure S14. 1D-TOCSY (4.70 ppm) spectrum of compound **1** in $CDCl_3$ 10
Figure S15. 1D-TOCSY (2.46 ppm) spectrum of compound **1** in $CDCl_3$ 11
Figure S16. HRESIMS data of compound **2** 11
Figure S17. IR spectrum of compound **2** 12
Figure S18. ECD spectrum of compound **2** 12
Figure S19. ^{1}H NMR spectrum of compound **2** in $CDCl_3$ 13
Figure S20. ^{13}C NMR spectrum of compound **2** in $CDCl_3$ 13
Figure S21. HSQC spectrum of compound **2** in $CDCl_3$ 14
Figure S22. ^{1}H-^{1}H COSY spectrum of compound **2** in $CDCl_3$ 14
Figure S23. HMBC spectrum of compound **2** in $CDCl_3$ 15
Figure S24. ROESY spectrum of compound **2** in $CDCl_3$ 15
Figure S25. Selective HSQC (C15-30) spectrum of compound **2** in $CDCl_3$ 16
Figure S26. Selective HSQC (C30-45) spectrum of compound **2** in $CDCl_3$ 16
Figure S27. Selective HMBC (C15-30) spectrum of compound **2** in $CDCl_3$ 17
Figure S28. Selective HMBC (C30-45) spectrum of compound **2** in $CDCl_3$ 17
Figure S29. 1D-TOCSY (4.29 ppm) spectrum of compound **2** in $CDCl_3$ 18
Figure S30. HRESIMS data of compound **3** 18
Figure S31. IR spectrum of compound **3** 19
Figure S32. ECD spectrum of compound **3** 19
Figure S33. ^{1}H NMR spectrum of compound **3** in $CDCl_3$ 20
Figure S34. ^{13}C NMR spectrum of compound **3** in $CDCl_3$ 20
Figure S35. HSQC spectrum of compound **3** in $CDCl_3$ 21
Figure S36. ^{1}H-^{1}H COSY spectrum of compound **3** in $CDCl_3$ 21
Figure S37. HMBC spectrum of compound **3** in $CDCl_3$ 22
Figure S38. ROESY spectrum of compound **3** in $CDCl_3$ 22
Figure S39. Selective HSQC (C15-30) spectrum of compound **3** in $CDCl_3$ 23

Figure S40. Selective HSQC (C30-45) spectrum of compound **3** in $CDCl_3$ 23
Figure S41. Selective HMBC (C15-30) spectrum of compound **3** in $CDCl_3$ 24
Figure S42. Selective HMBC (C28-45) spectrum of compound **3** in $CDCl_3$ 24
Figure S43. 1D-TOCSY (4.64 ppm) spectrum of compound **3** in $CDCl_3$ 25
Figure S44. 1D-TOCSY (4.76 ppm) spectrum of compound **3** in $CDCl_3$ 25
Figure S45. 1D-TOCSY (4.56 ppm) spectrum of compound **3** in $CDCl_3$ 26
Table S1. Cytotoxicity of Compounds **1**, **2**, and **3** against CCRF-CEM and HCT-116 Cell Lines 26
Cytotoxicity Assays 26
Computational details 27
Table S2. Calculated DFT free energies of four diastereoisomers (6′R*11″R*,6′R*11″S*, 6′S*11″R*, and 6′S*11″S*) of compound **3** 28
Table S3. Comparison between computational and experimental ^{13}C chemical shifts for four diastereoisomers (6′R*11″R*,6′R*11″S*, 6′S*11″R*, and 6’S*11’’S*) of **3** 29
Table S4. Comparison between computational and experimental ^{1}H chemical shifts for four diastereoisomers (6′R*11″R*, 6′R*11″S*, 6′S*11″R*, and 6′S*11″S*) of **3** 30
Table S5. DP4+ correlations for four diastereoisomers of **3** : 6′R*11″R* (Isomer 1), 6′R*11″S* (Isomer 2), 6′S*11″R* (Isomer 3), 6′S*11″S* (Isomer 4) 31
Figure S46. ^{1}H-NMR correlation for four diasteroisomers of **3**. 32
Figure S47. ^{13}C-NMR correlation for four diasteroisomers of **3**. 32
Table S6. Calculated DFT free energies of two diastereoisomers (11′R* and 11′S*) of **1**. 33
Table S7. Comparison between computational and experimental ^{13}C chemical shifts for two diastereoisomers (11′R* and 11′S*) of **1**. 34
Table S8. Comparison between computational and experimental ^{1}H chemical shifts for two diastereoisomers (11′R* and 11′S*) of **1**. 35
Table S9. DP4+ correlations for two diastereoisomers of **1** : 11′R* (Isomer 1), and 11′S* (Isomer 2). 36
Figure S48. ^{1}H-NMR correlation for two diasteroisomers of **1**. 36
Figure S49. ^{13}C-NMR correlation for two diasteroisomers of **1**. 36
References 37

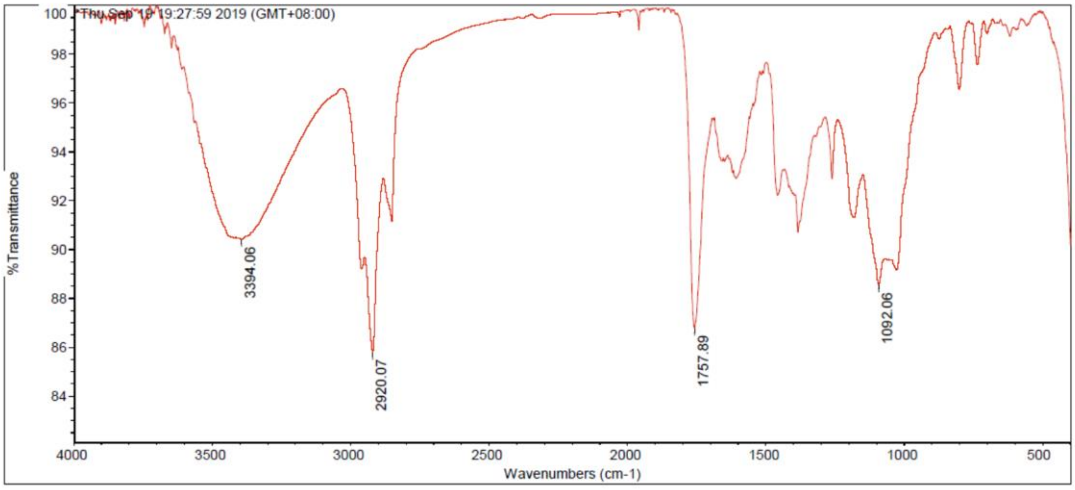

Thu Sep 19 19:31:07 2019 (GMT+08:00)
FIND PEAKS:

Spectrum:	*Thu Sep 19 19:27:59 2019 (GMT+08:00)		
Region:	4000.00	400.00	
Absolute threshold:	90.433		
Sensitivity:	50		
Peak list:			
Position:	1092.06	Intensity:	88.575
Position:	1757.89	Intensity:	86.778
Position:	2920.07	Intensity:	85.796
Position:	3394.06	Intensity:	90.419

Figure S1. IR spectrum of compound **1**

Elemental Composition Report
Tolerance = 5.0 PPM / DBE: min = -1.5, max = 50.0
Element prediction: Off
Number of isotope peaks used for i-FIT = 3
Monoisotopic Mass, Even Electron Ions
320 formula(e) evaluated with 1 results within limits (up to 50 best isotopic matches for each mass)
Elements Used:
C: 0-80 H: 0-100 N: 0-1 O: 0-20

Minimum:	80.00					-1.5			
Maximum:	100.00		3.0	5.0		50.0			
Mass	RA	Calc. Mass	mDa	PPM		DBE	i-FIT	Norm	Conf(%) Formula
737.4631	100.00	737.4629	0.2	0.3	12.5	147.1	n/a	n/a	C44 H65 O9

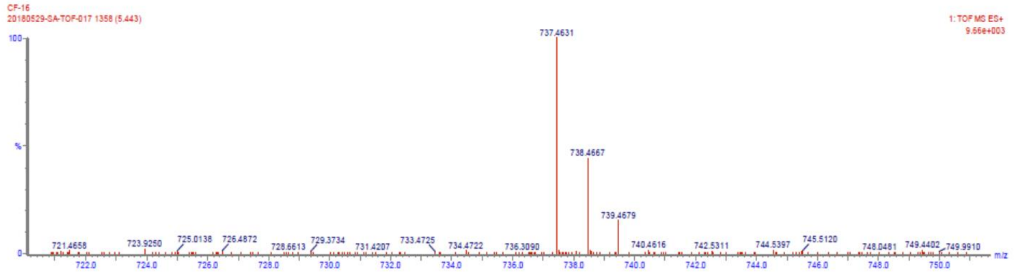

Figure S2. HRESIMS spectrum of compound **1**

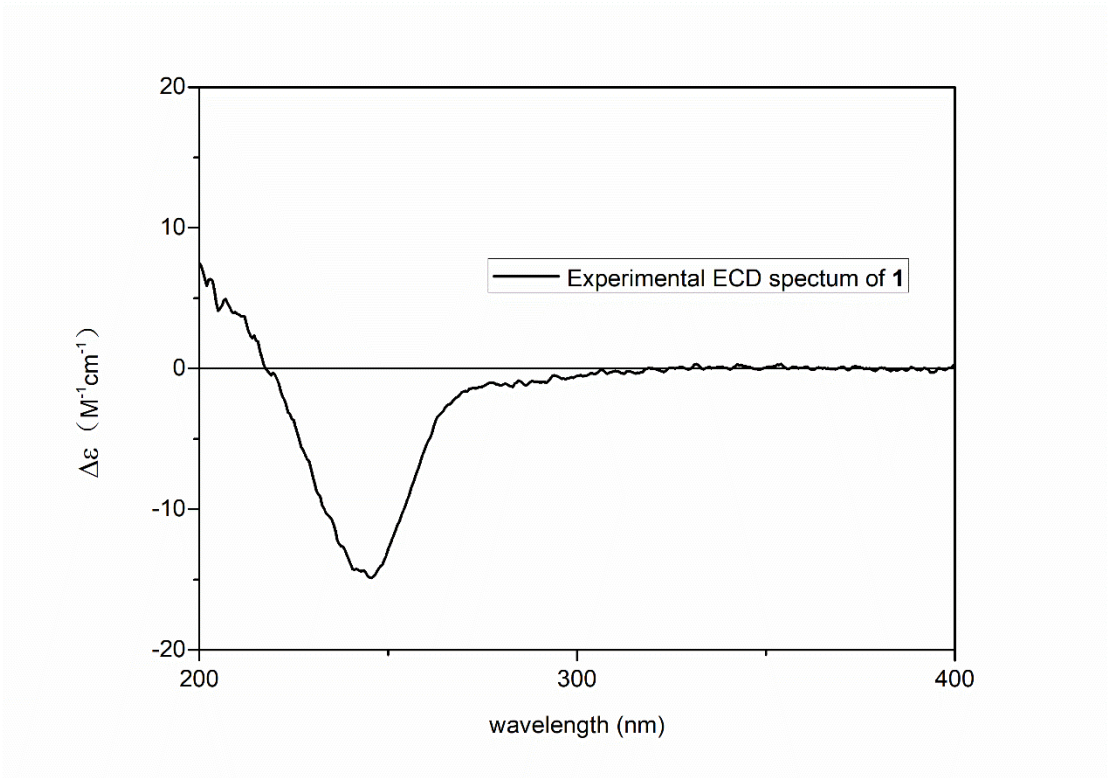

Figure S3. ECD spectrum of compound **1**

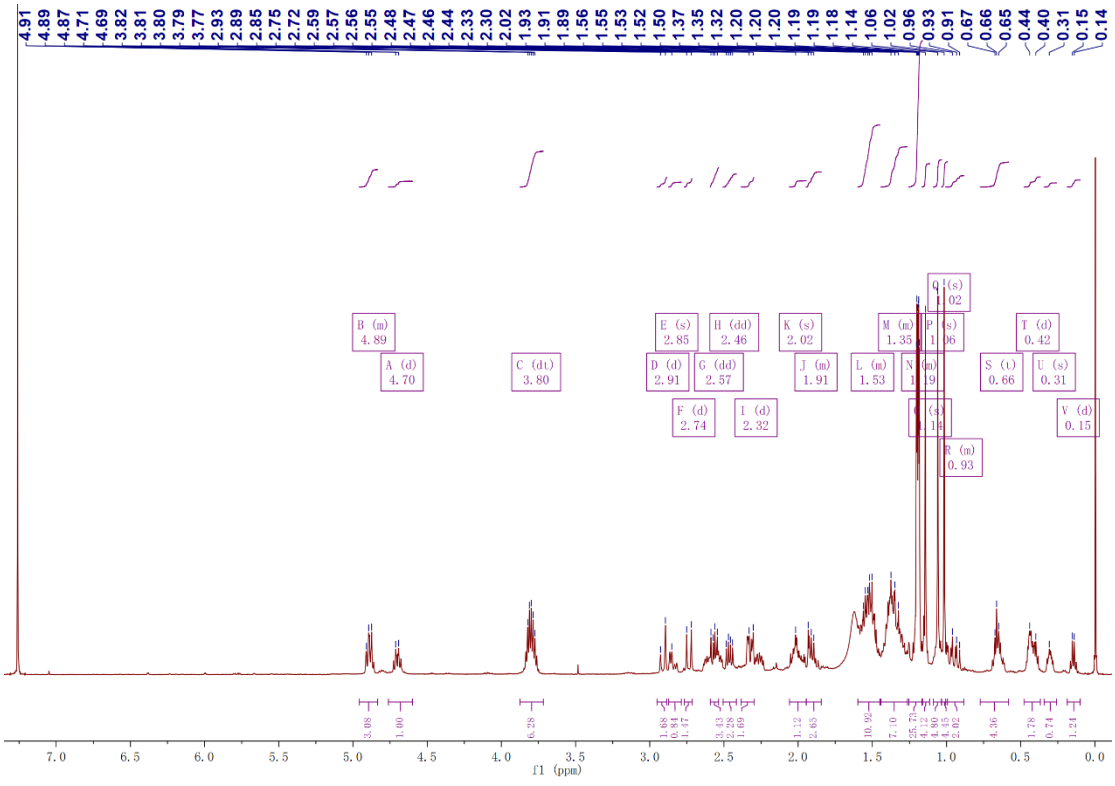

Figure S4. ^{1}H NMR spectrum of compound **1** in $CDCl_3$

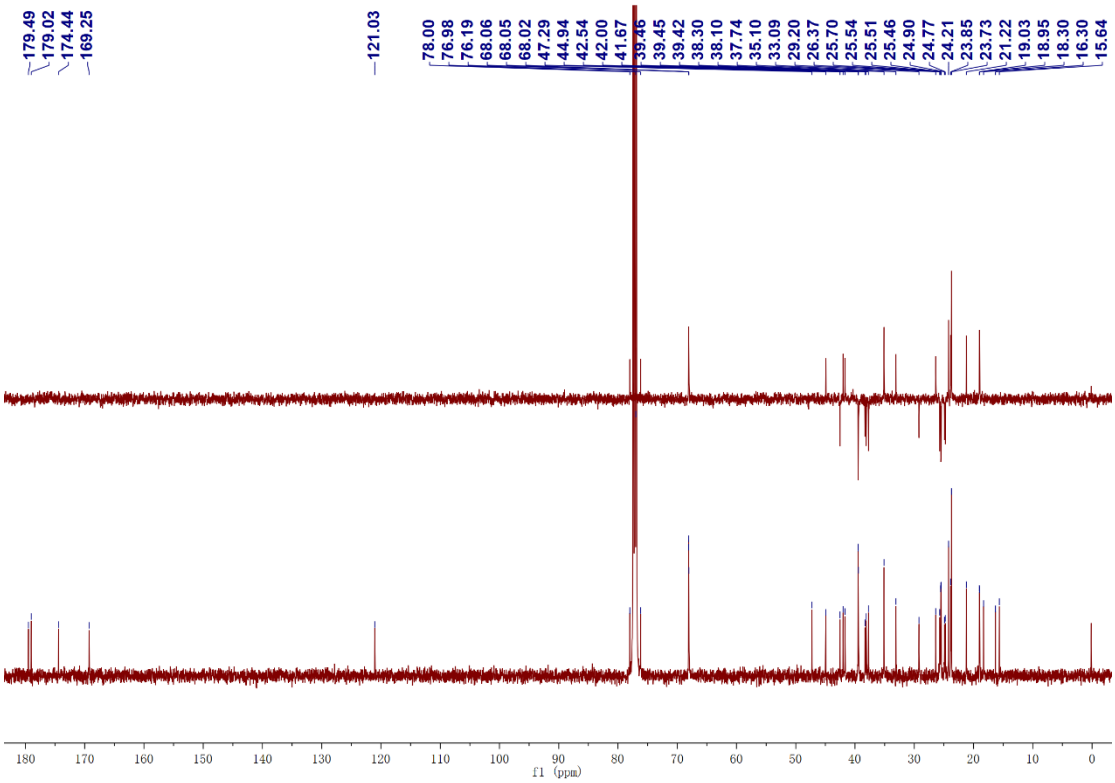

Figure S5. ^{13}C NMR and DEPT spectrum of compound **1** in $CDCl_3$

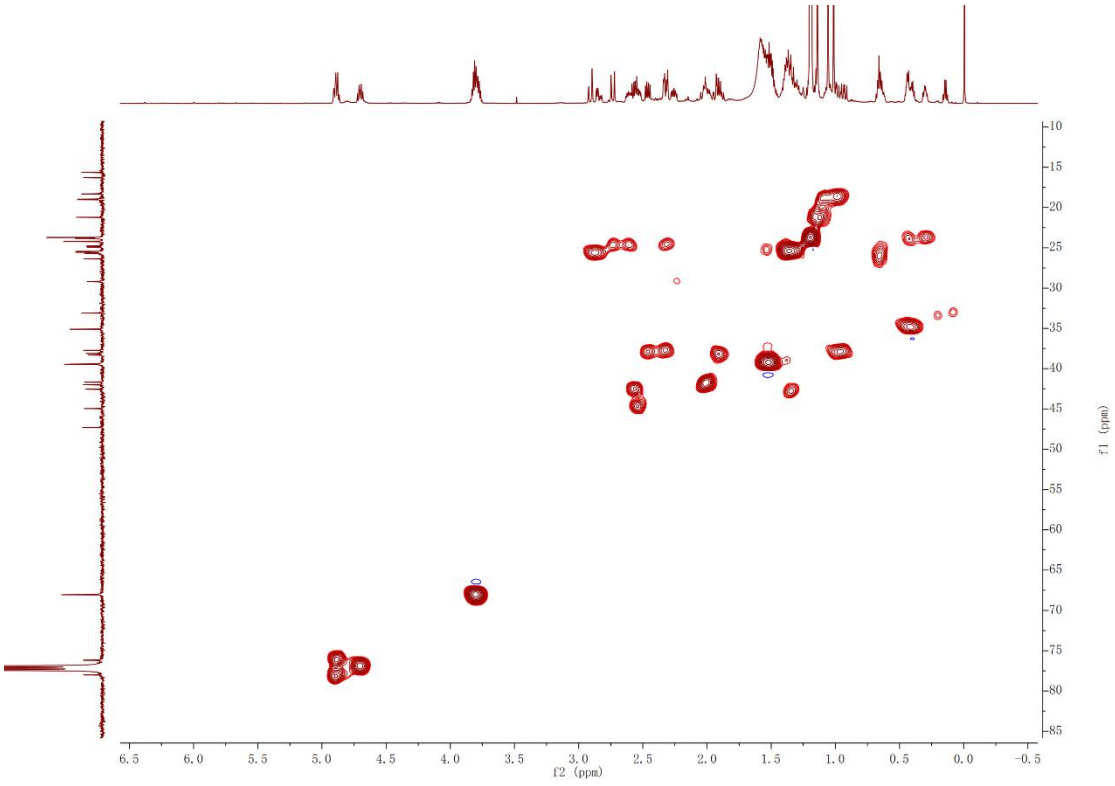

Figure S6. HSQC spectrum of compound **1** in $CDCl_3$

Figure S7. HMBC spectrum of compound **1** in $CDCl_3$

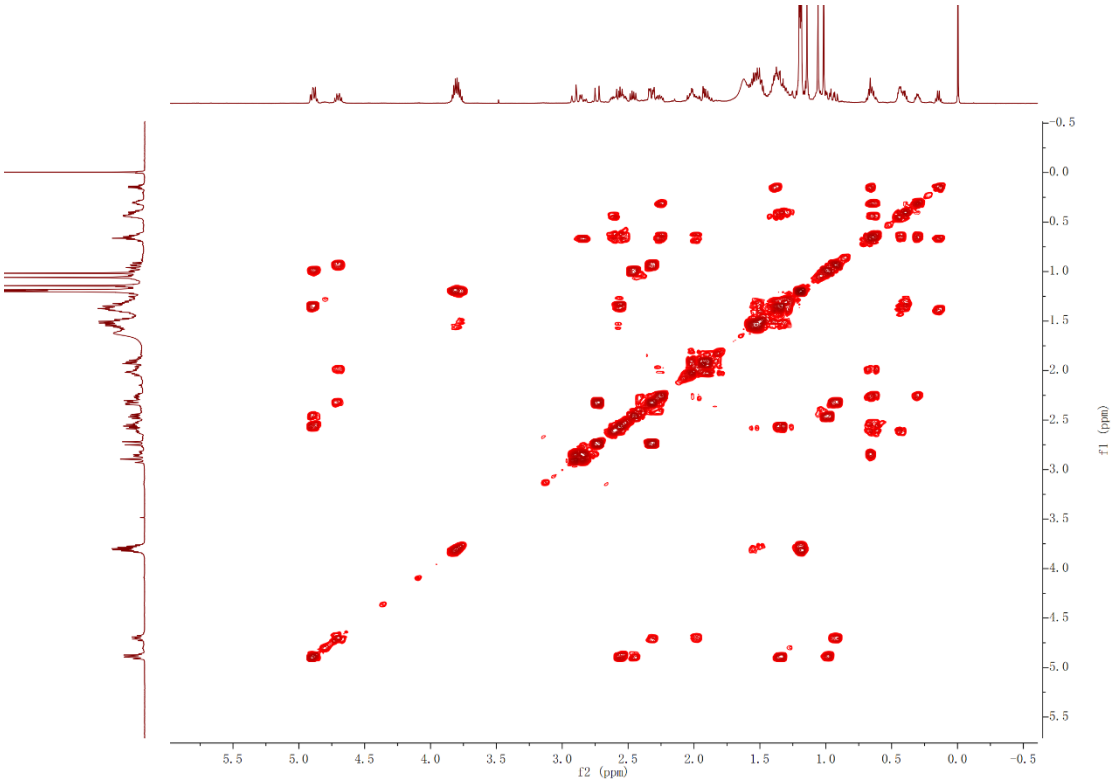

Figure S8. ^{1}H-^{1}H COSY spectrum of compound **1** in $CDCl_3$

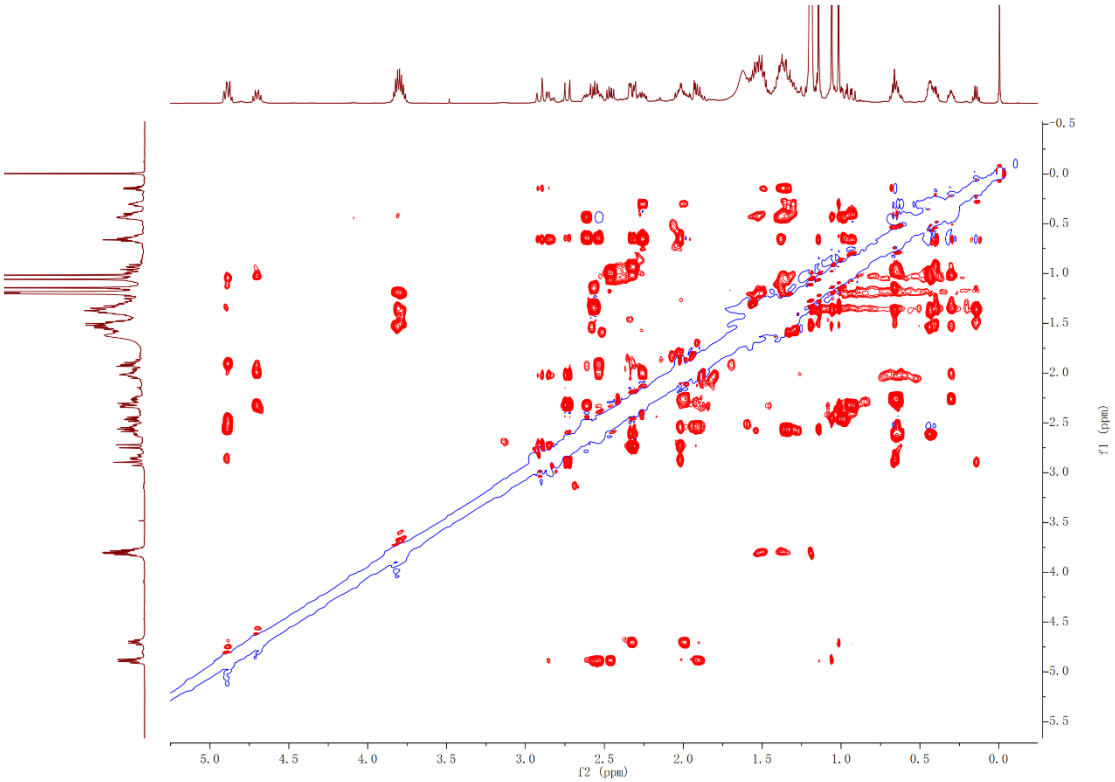

Figure S9. ROESY spectrum of compound **1** in $CDCl_3$

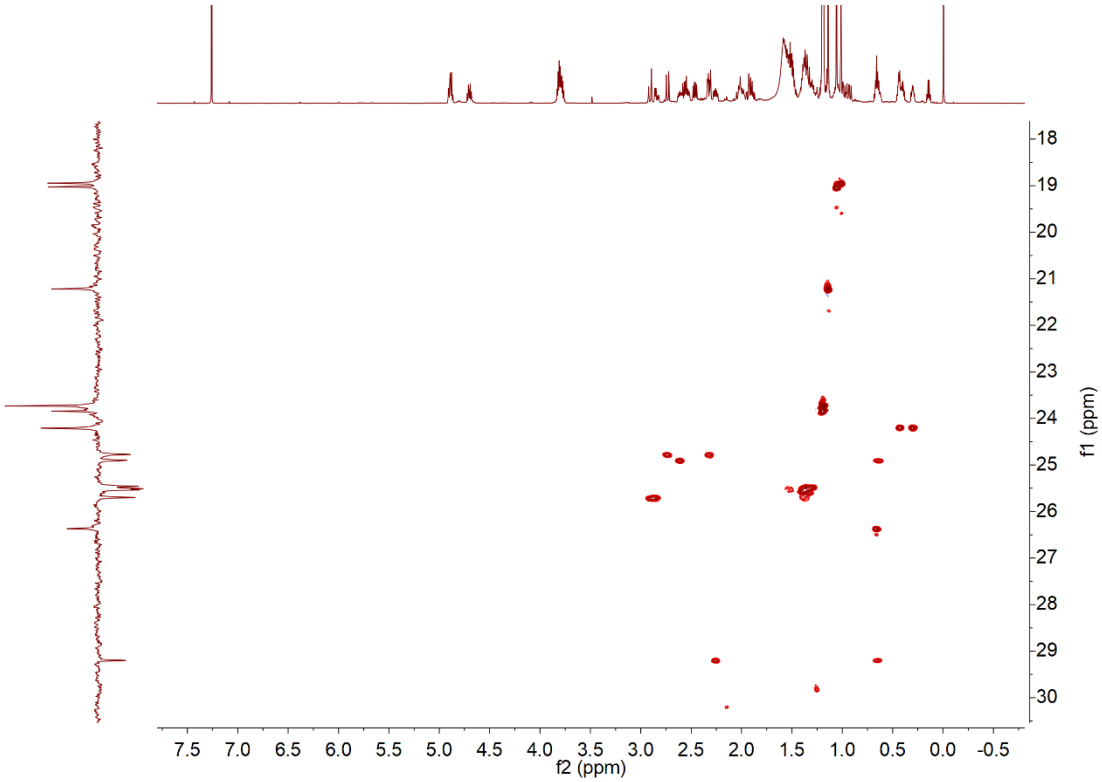

Figure S10. Selective HSQC (C15-30) spectrum of compound **1** in $CDCl_3$

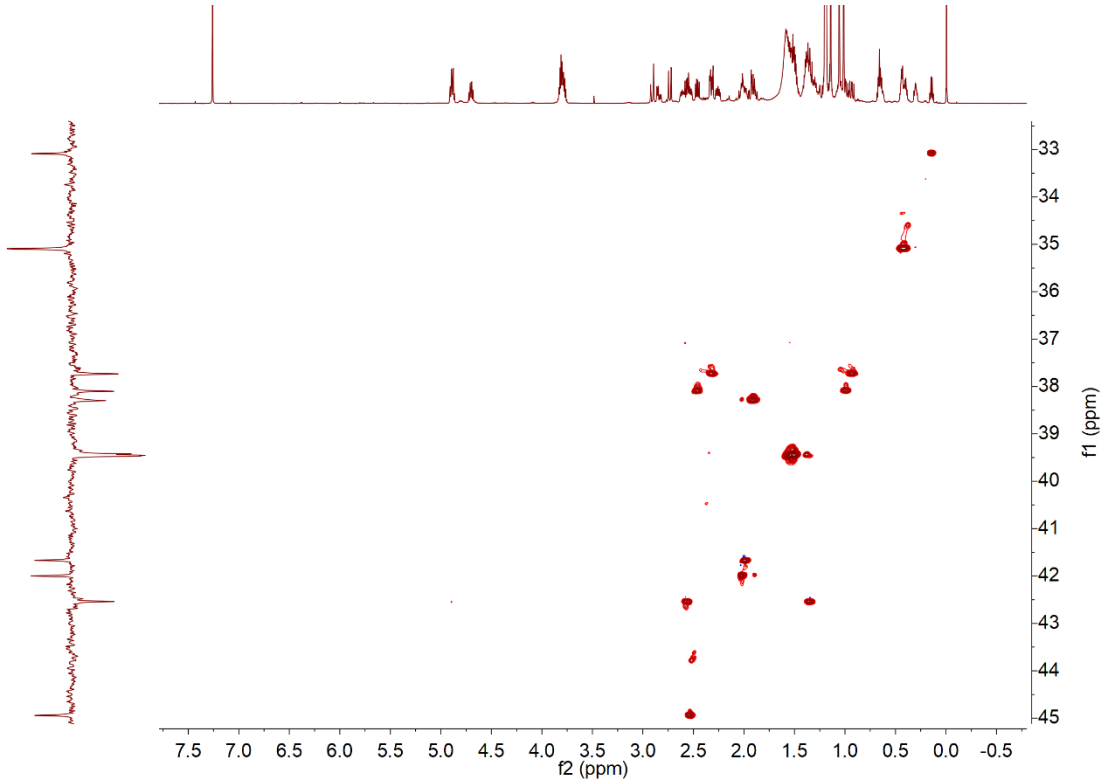

Figure S11. Selective HSQC (C30-45) spectrum of compound **1** in $CDCl_3$

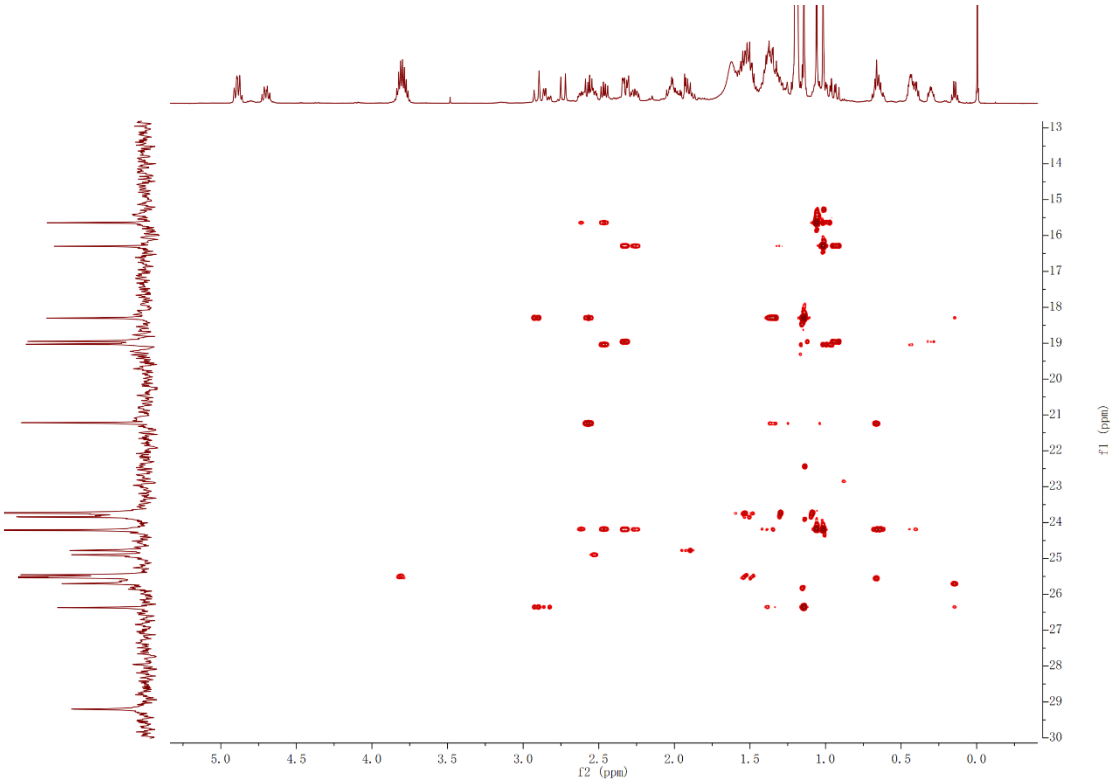

Figure S12. Selective HMBC (C15-30) spectrum of compound **1** in $CDCl_3$

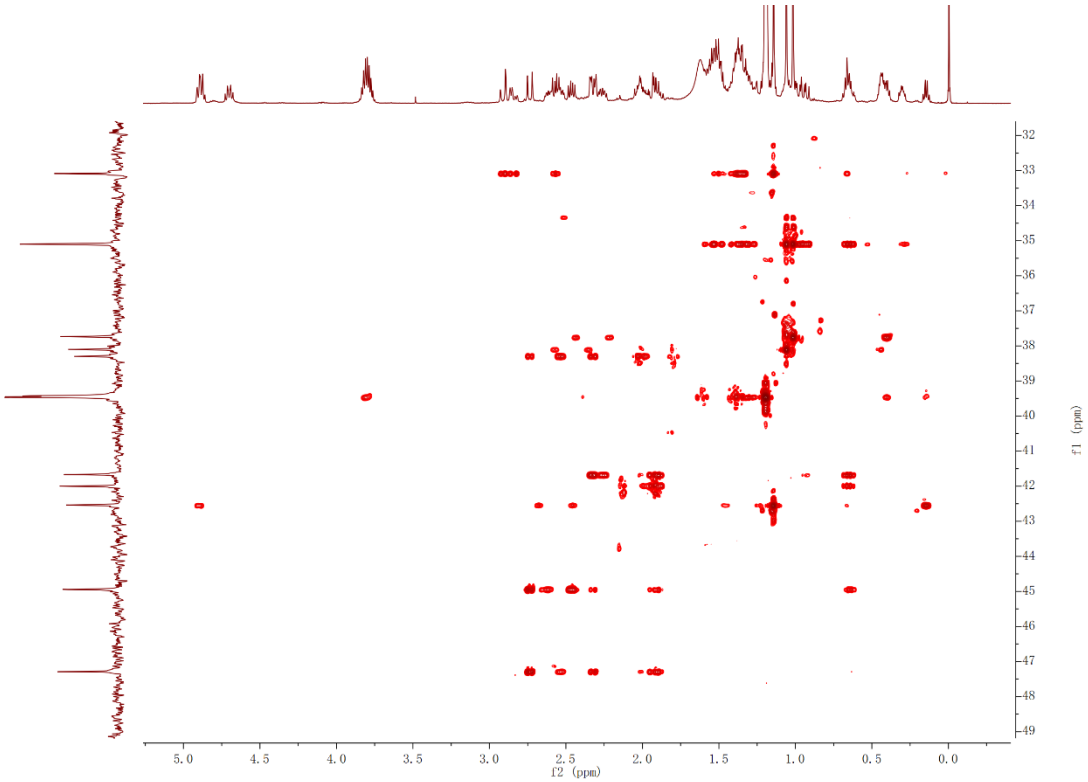

Figure S13. Selective HMBC (C30-45) spectrum of compound **1** in $CDCl_3$

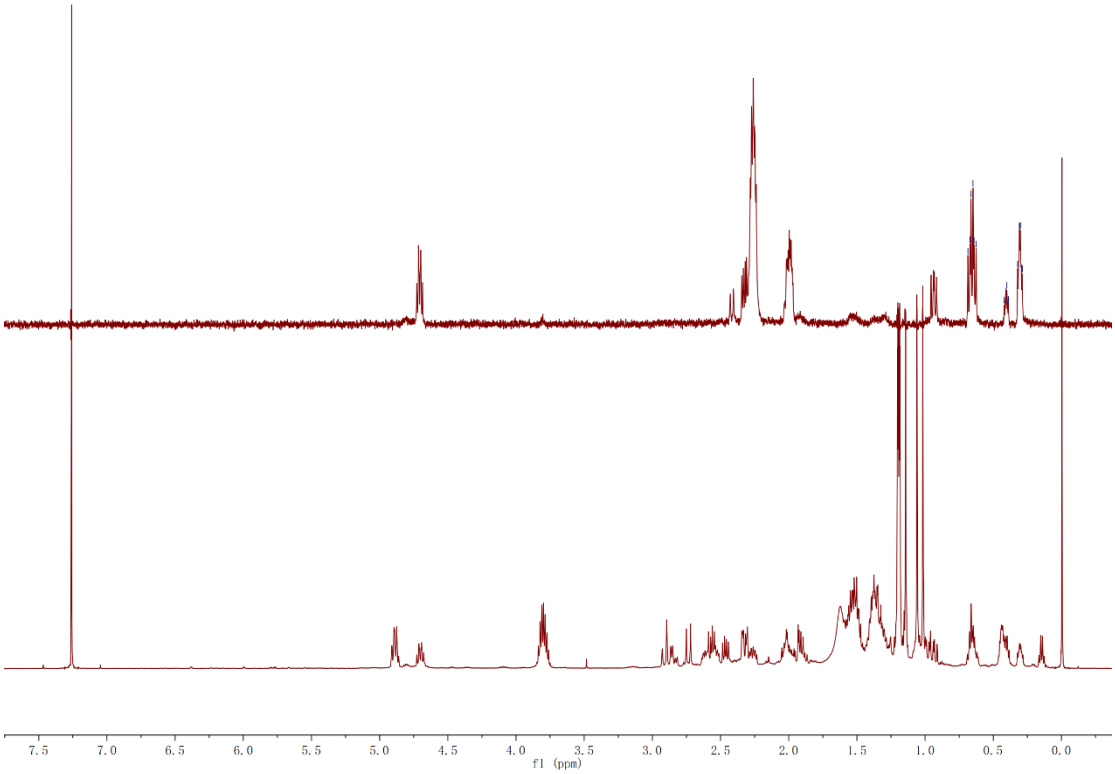

Figure S14. 1D-TOCSY (4.70 ppm) spectrum of compound **1** in $CDCl_3$

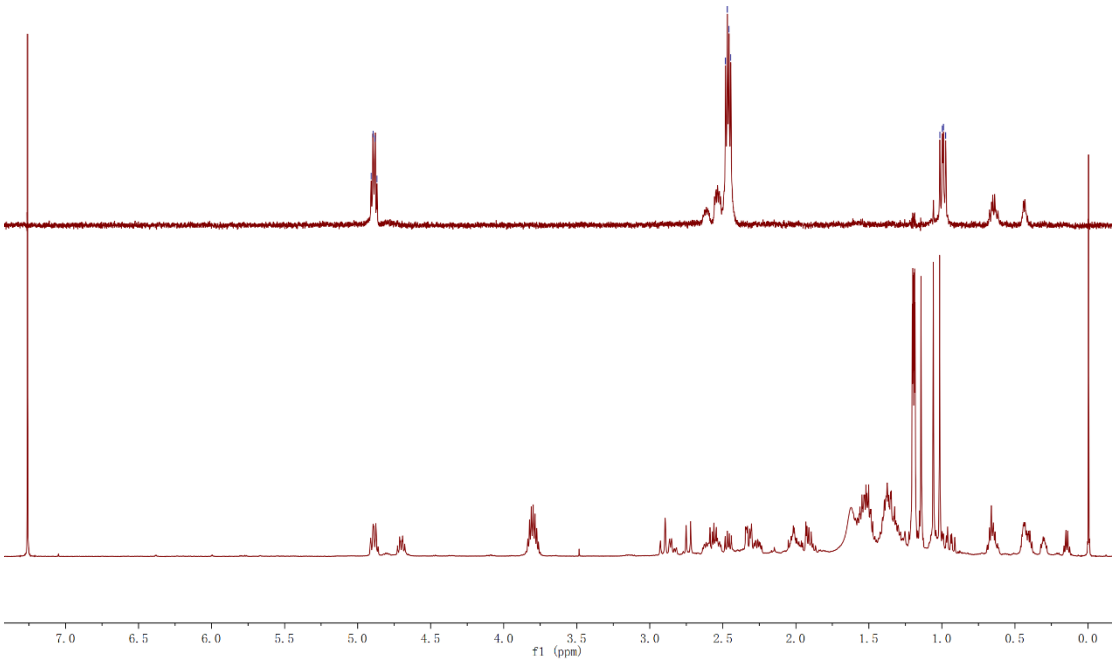

Figure S15. 1D-TOCSY (2.46 ppm) spectrum of compound **1** in $CDCl_3$

Elemental Composition Report

Tolerance = 5.0 PPM / DBE: min = -1.5, max = 50.0

Element prediction: Off

Number of isotope peaks used for i-FIT = 3

Monoisotopic Mass, Even Electron Ions

320 formula(e) evaluated with 1 results within limits (up to 50 best isotopic matches for each mass)

Elements Used:

C: 0-80 H: 0-100 N: 0-1 O: 0-20

Minimum:	80.00					-1.5				
Maximum:	100.00			3.0	5.0	50.0				
Mass	RA	Calc. Mass	mDa	PPM		DBE	i-FIT	Norm	Conf(%)	Formula
737.4634	100.00	737.4629	0.5	0.7	12.5	322.5	n/a	n/a		C44 H65 O9

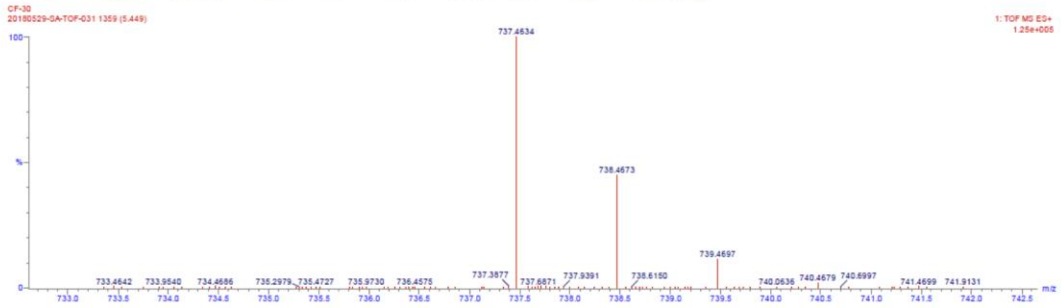

Figure S16. HRESIMS data of compound **2**

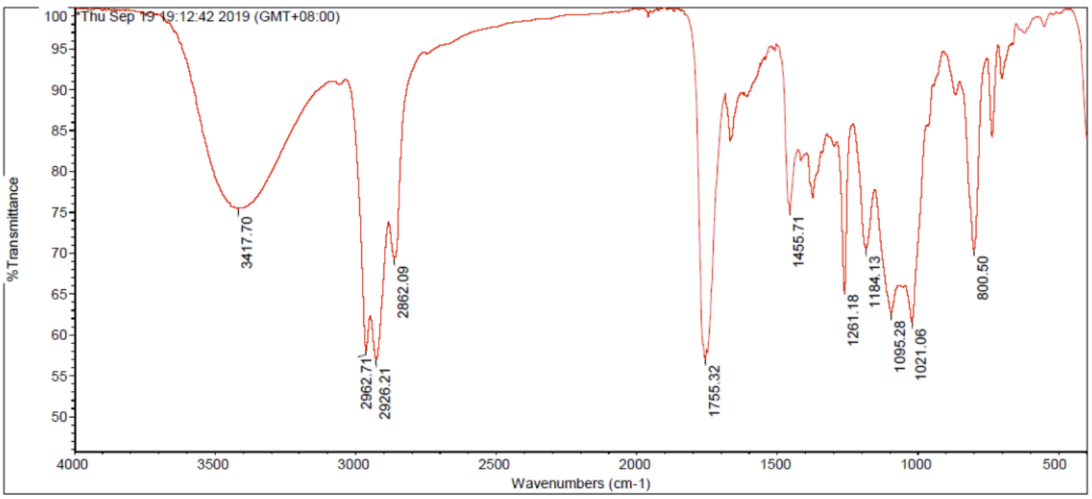

Thu Sep 19 19:16:09 2019 (GMT+08:00)
FIND PEAKS:
Spectrum: *Thu Sep 19 19:12:42 2019 (GMT+08:00)
Region: 4000.00 400.00
Absolute threshold: 75.548
Sensitivity: 50
Peak list:

Position:	800.50	Intensity:	70.305	Position:	2862.09	Intensity:	69.404
Position:	1021.06	Intensity:	61.534	Position:	2926.21	Intensity:	56.924
Position:	1095.28	Intensity:	62.716	Position:	2962.71	Intensity:	58.072
Position:	1184.13	Intensity:	70.557	Position:	3417.70	Intensity:	75.444
Position:	1261.18	Intensity:	65.172				
Position:	1455.71	Intensity:	74.942				
Position:	1755.32	Intensity:	57.037				

Figure S17. IR spectrum of compound **2**

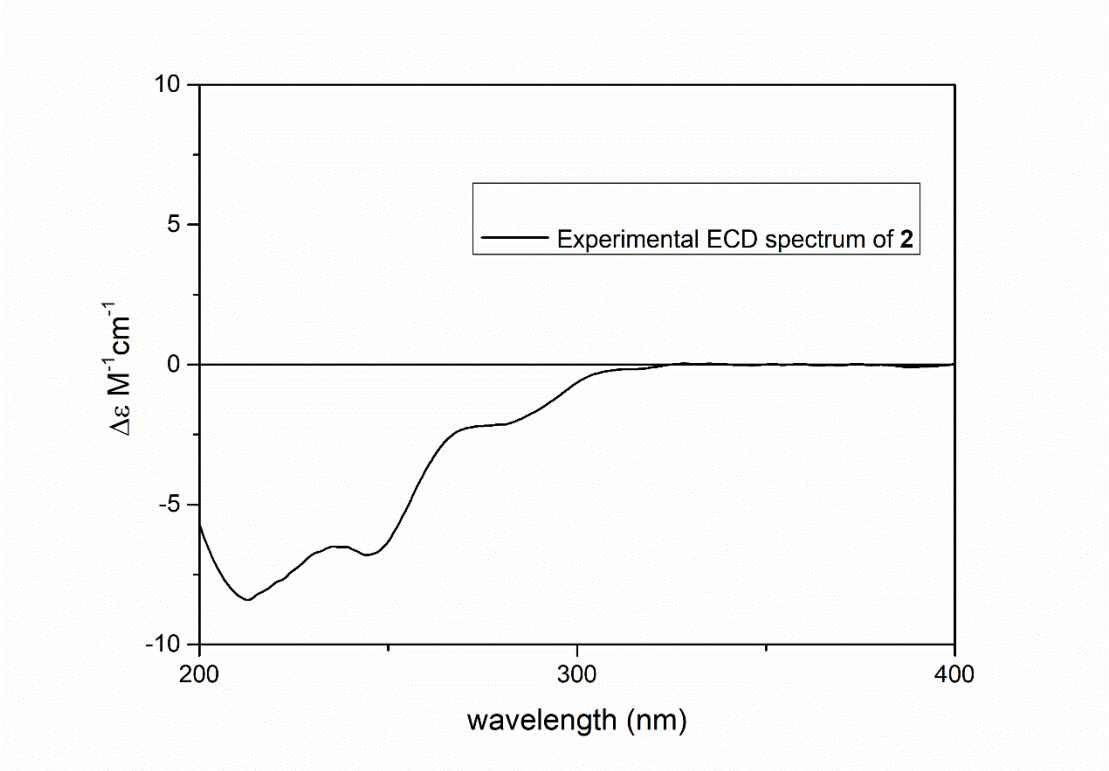

Figure S18. ECD spectrum of compound **2**

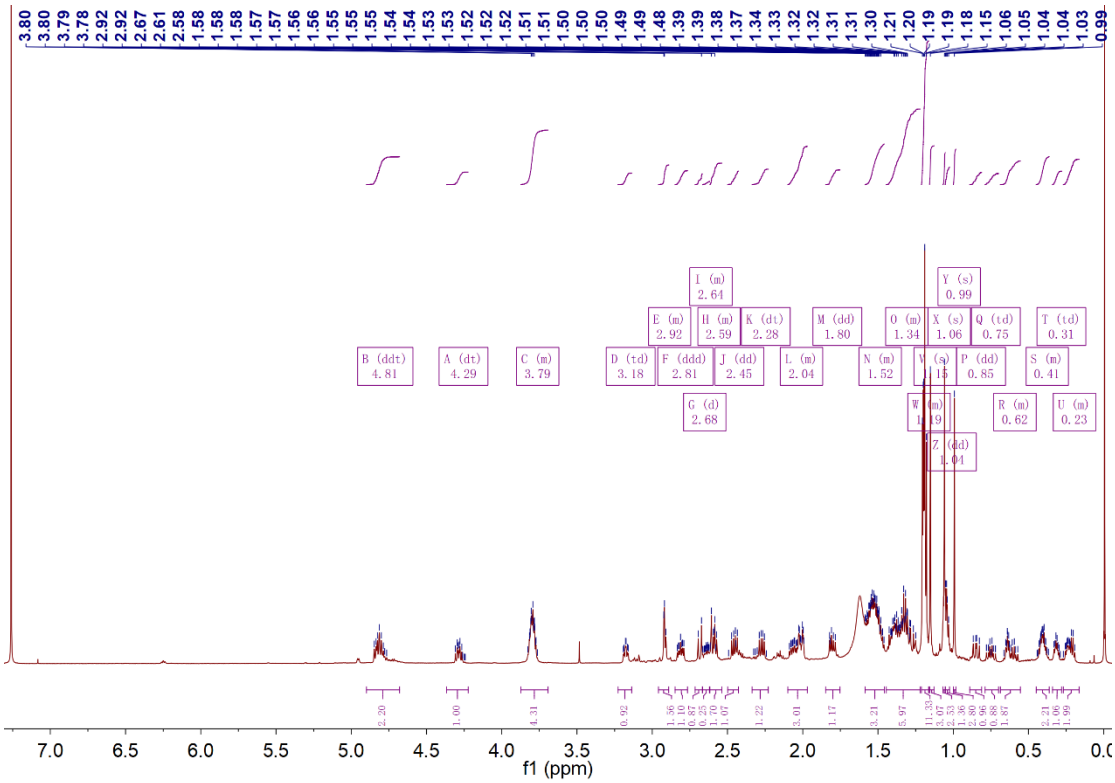

Figure S19. ^{1}H NMR spectrum of compound **2** in $CDCl_3$

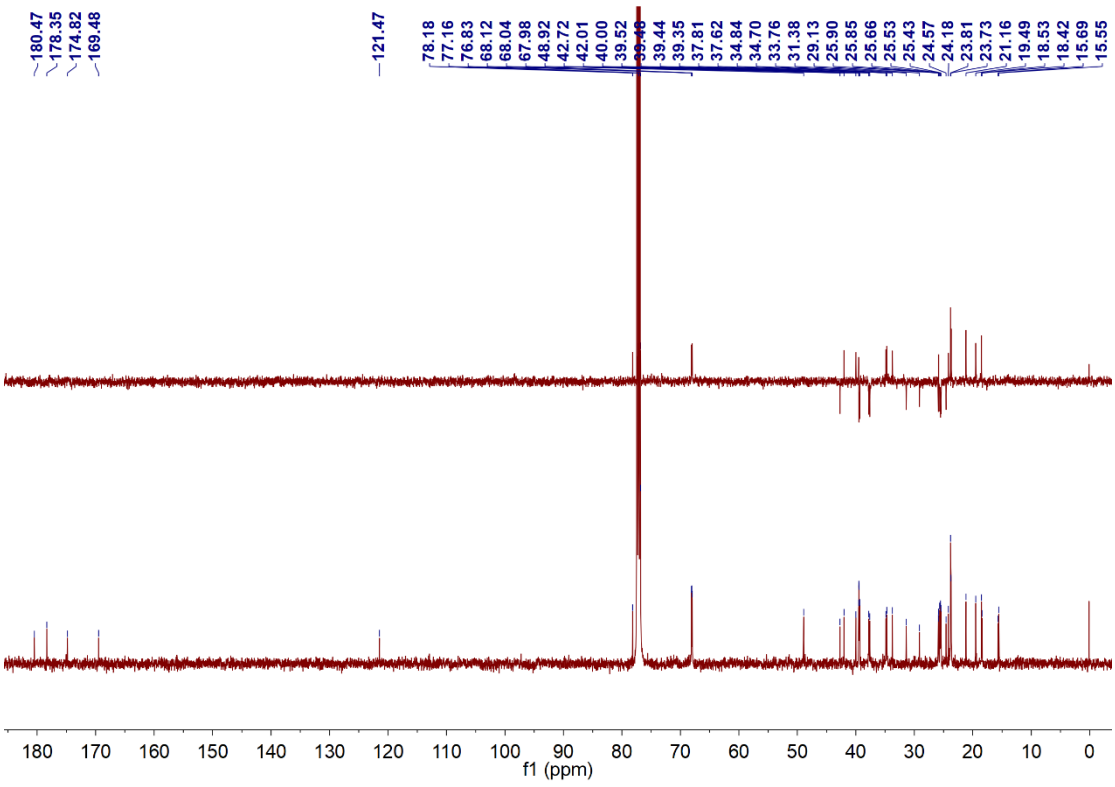

Figure S20. ^{13}C NMR spectrum of compound **2** in $CDCl_3$

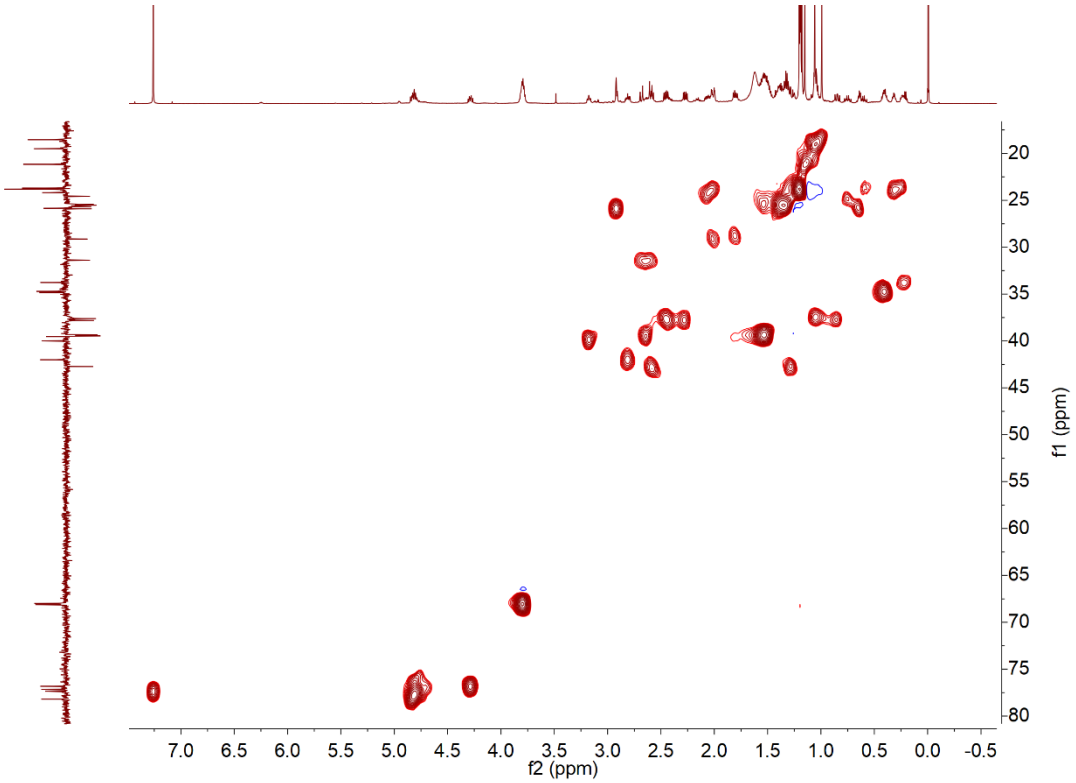

Figure S21. HSQC spectrum of compound **2** in $CDCl_3$

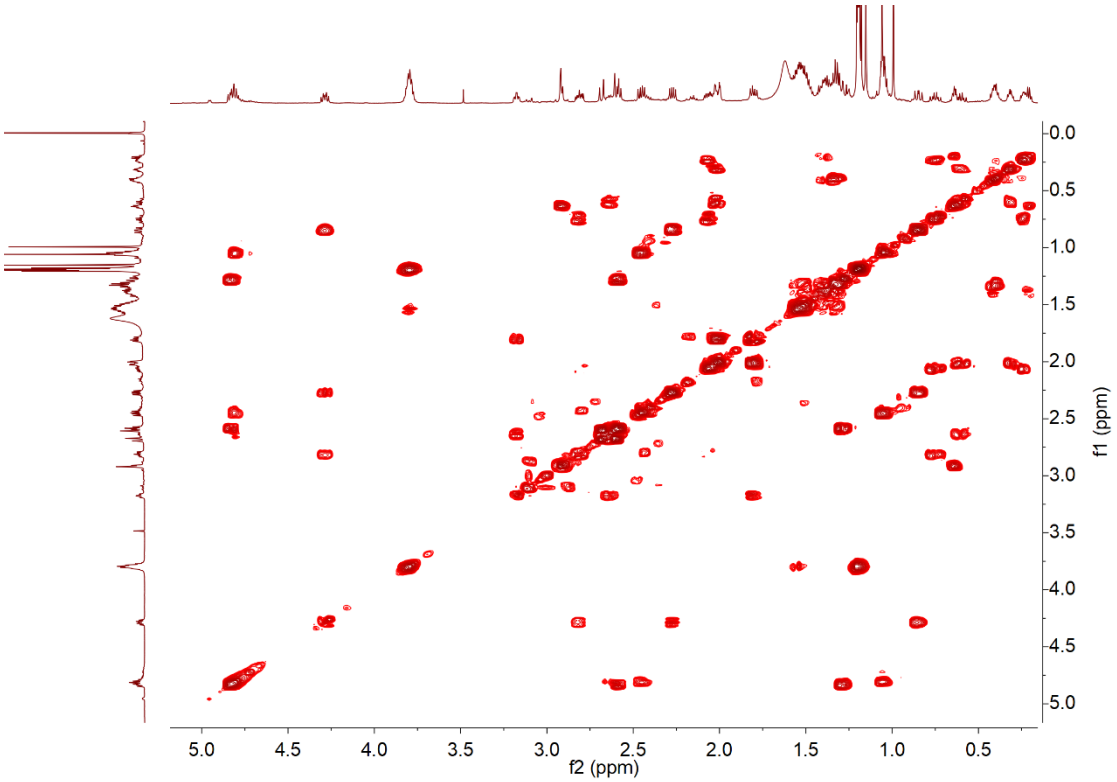

Figure S22. ^{1}H-^{1}H COSY spectrum of compound **2** in $CDCl_3$

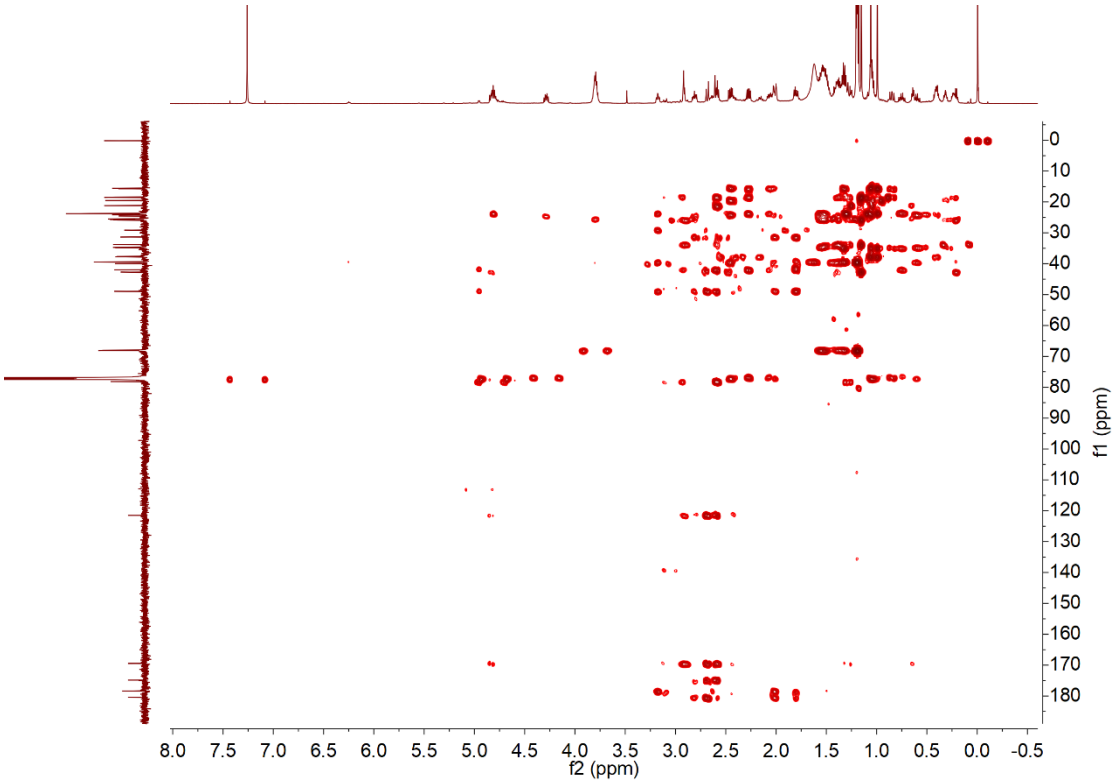

Figure S23. HMBC spectrum of compound **2** in $CDCl_3$

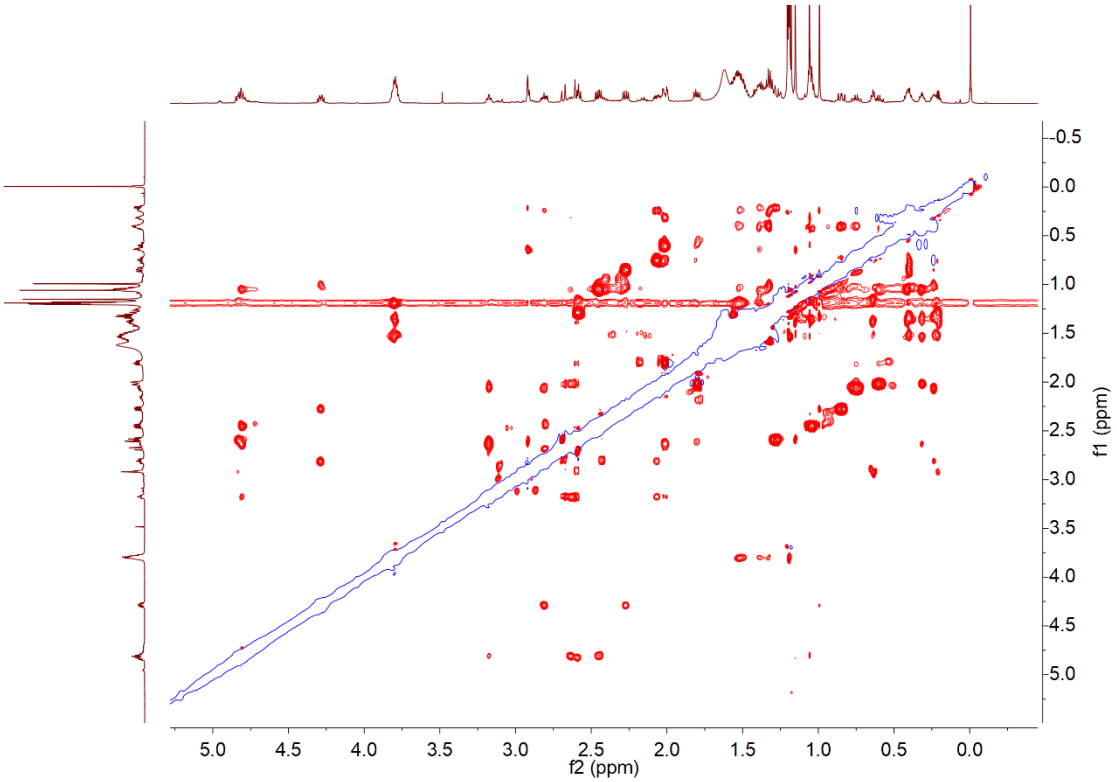

Figure S24. ROESY spectrum of compound **2** in $CDCl_3$

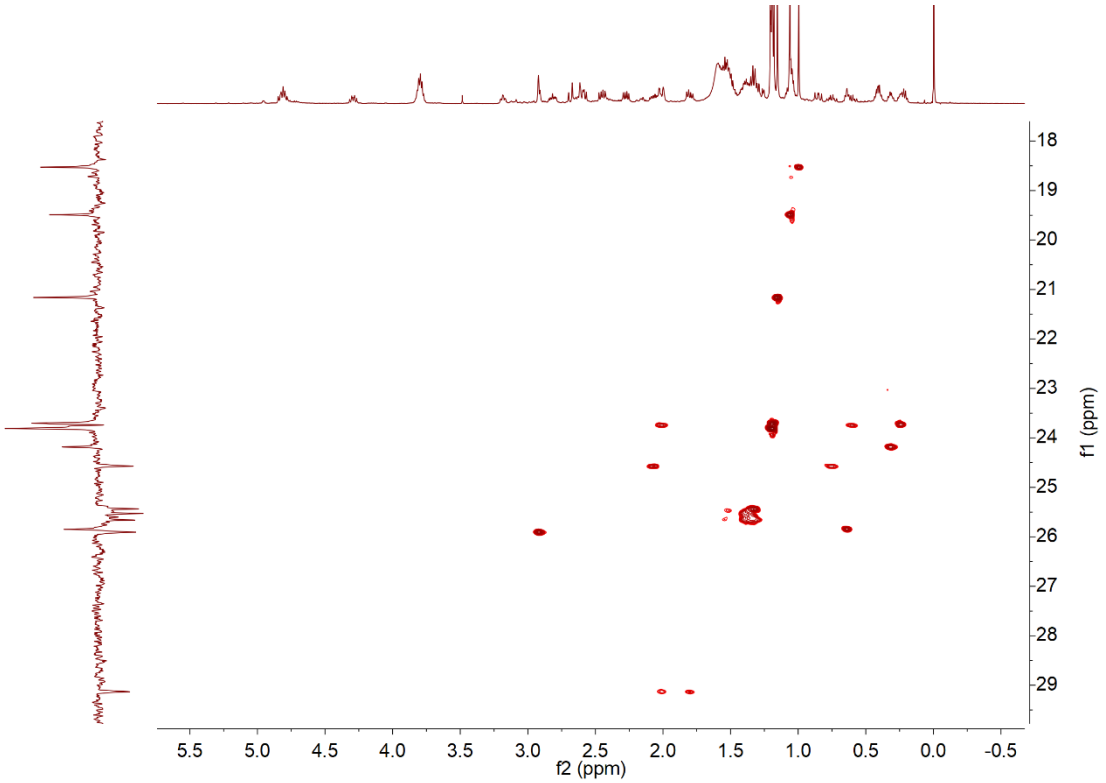

Figure S25. Selective HSQC (C15-30) spectrum of compound **2** in $CDCl_3$

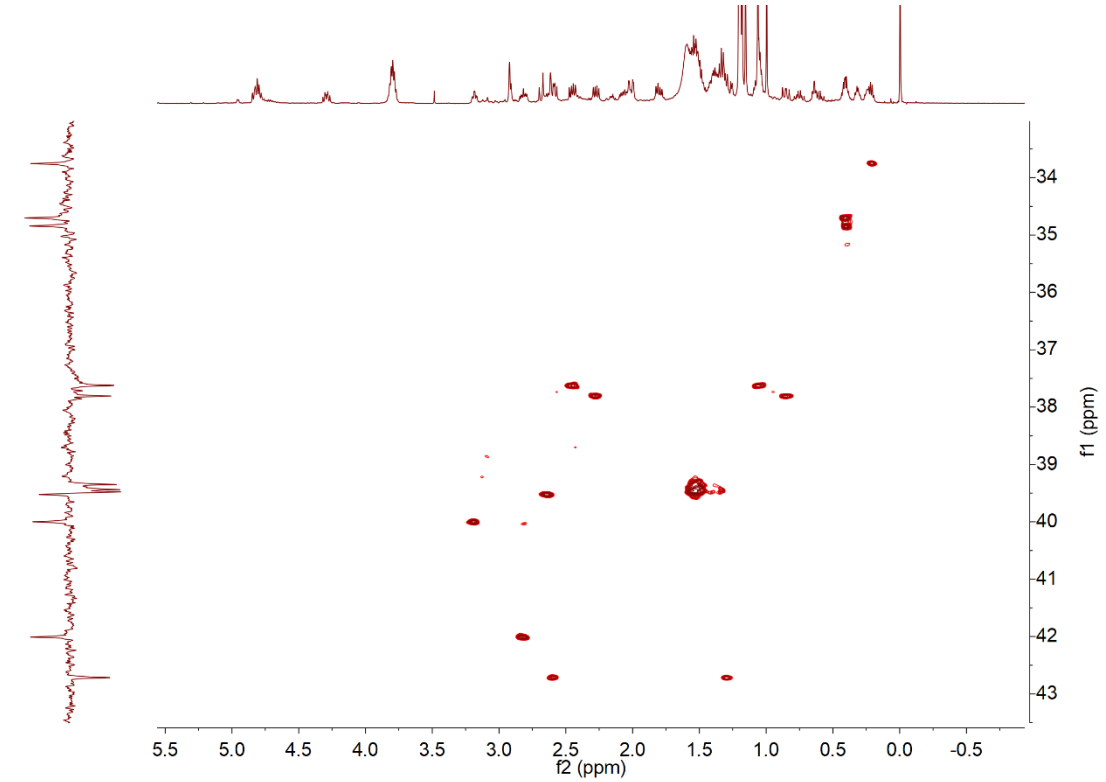

Figure S26. Selective HSQC (C30-45) spectrum of compound **2** in $CDCl_3$

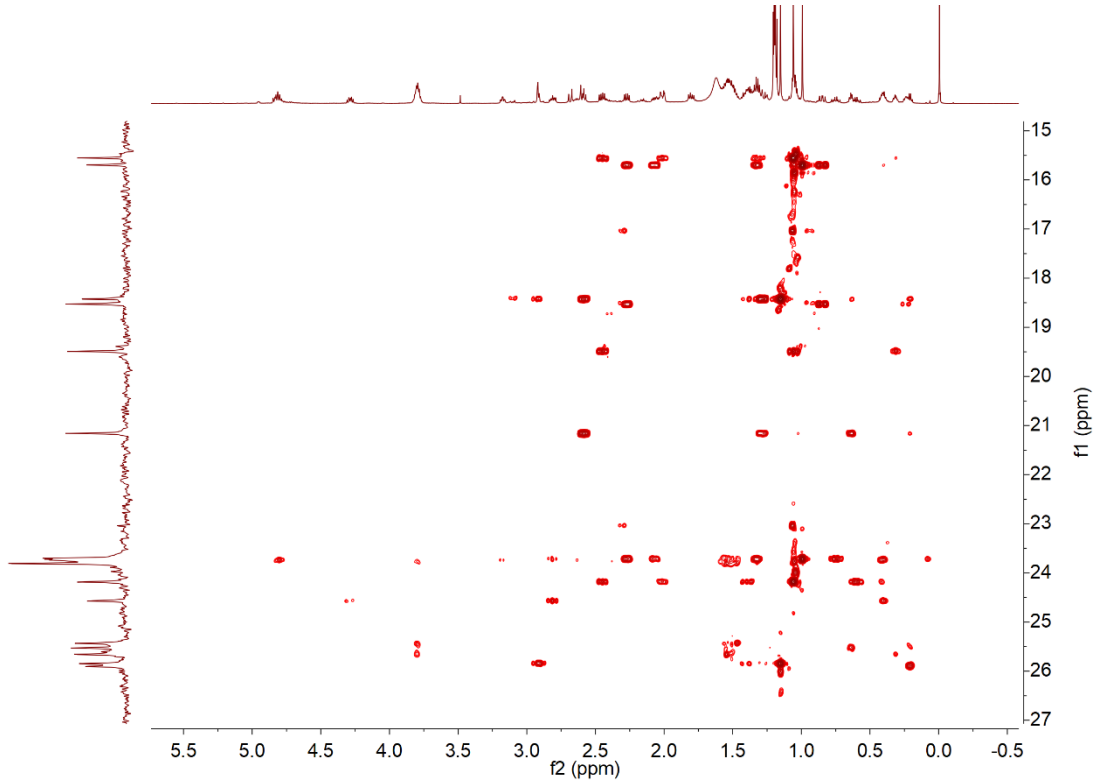

Figure S27. Selective HMBC (C15-30) spectrum of compound **2** in $CDCl_3$

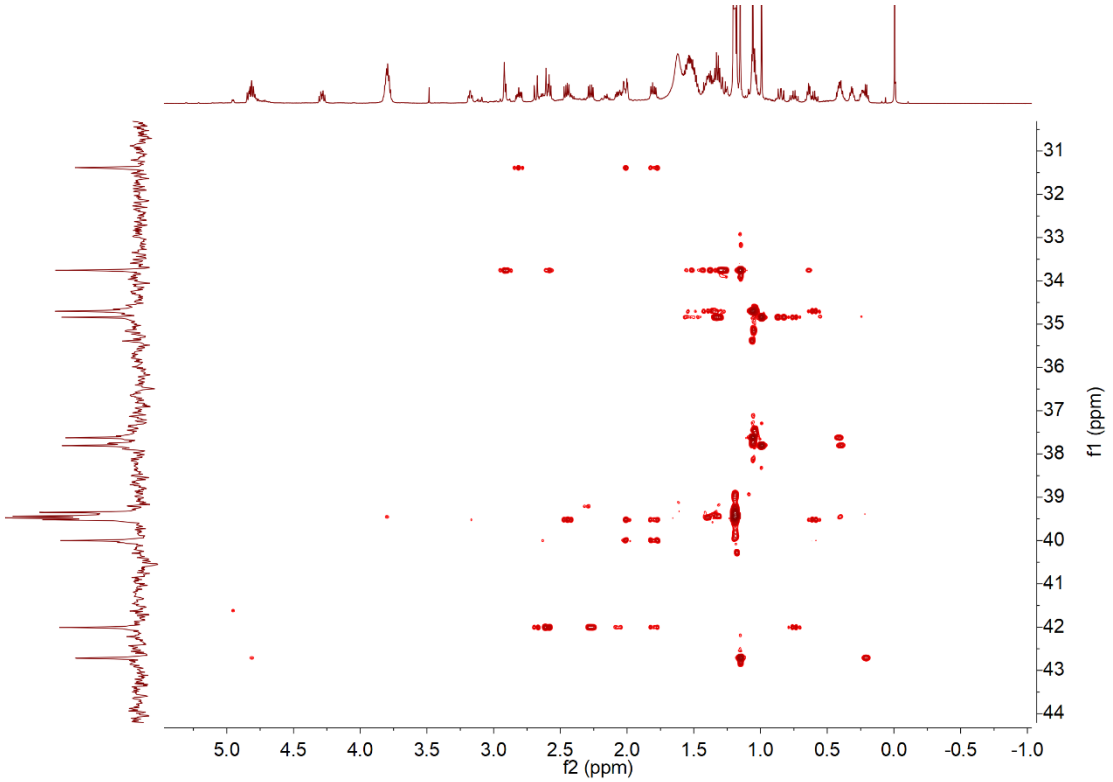

Figure S28. Selective HMBC (C30-45) spectrum of compound **2** in $CDCl_3$

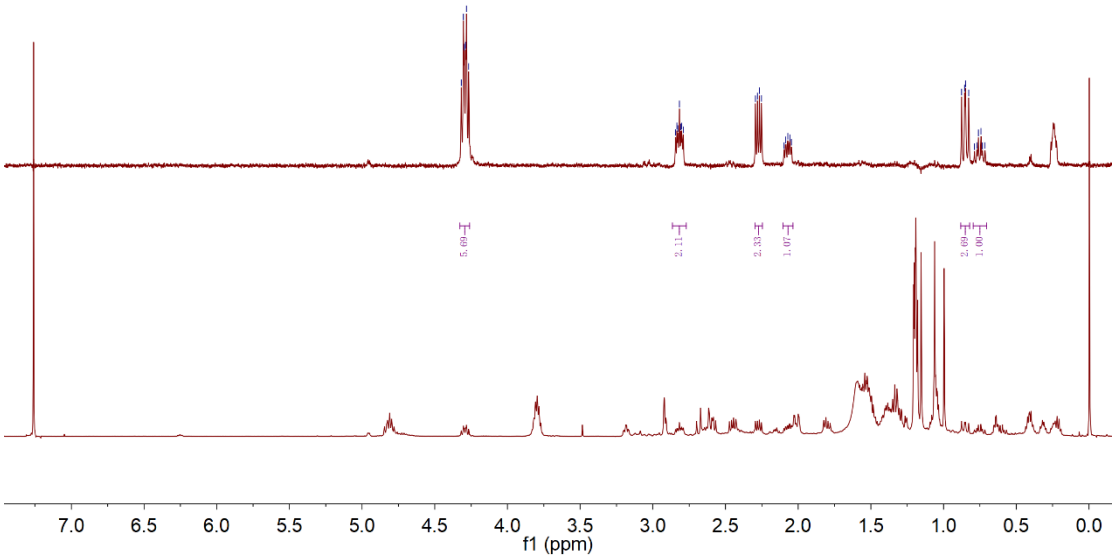

Figure S29. 1D-TOCSY (4.29 ppm) spectrum of compound **2** in $CDCl_3$

Elemental Composition Report

Tolerance = 5.0 PPM / DBE: min = -1.5, max = 50.0

Element prediction: Off

Number of isotope peaks used for i-FIT = 3

Monoisotopic Mass, Even Electron Ions

324 formula(e) evaluated with 1 results within limits (up to 50 best isotopic matches for each mass)

Elements Used:

C: 0-80 H: 0-100 N: 0-1 O: 0-20

Minimum:	80.00					-1.5				
Maximum:	100.00			3.0	5.0	50.0				
Mass	RA	Calc. Mass	mDa	PPM		DBE	i-FIT	Norm	Conf(%)	Formula
751.4785	100.00	751.4785	0.0	0.0	12.5	99.4	n/a	n/a		C45 H67 O9

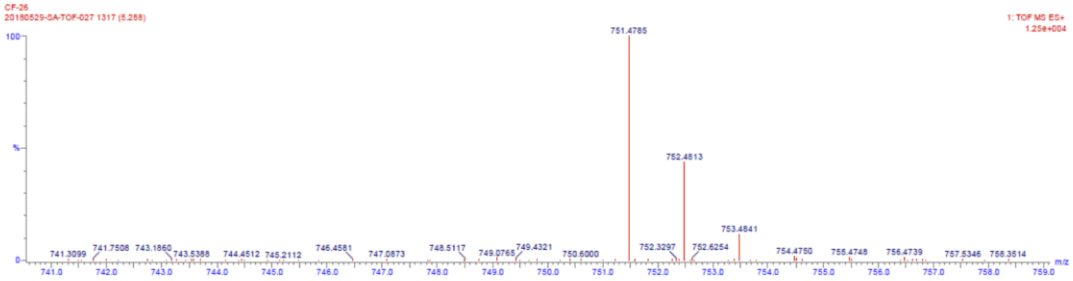

Figure S30. HRESIMS data of compound **3**

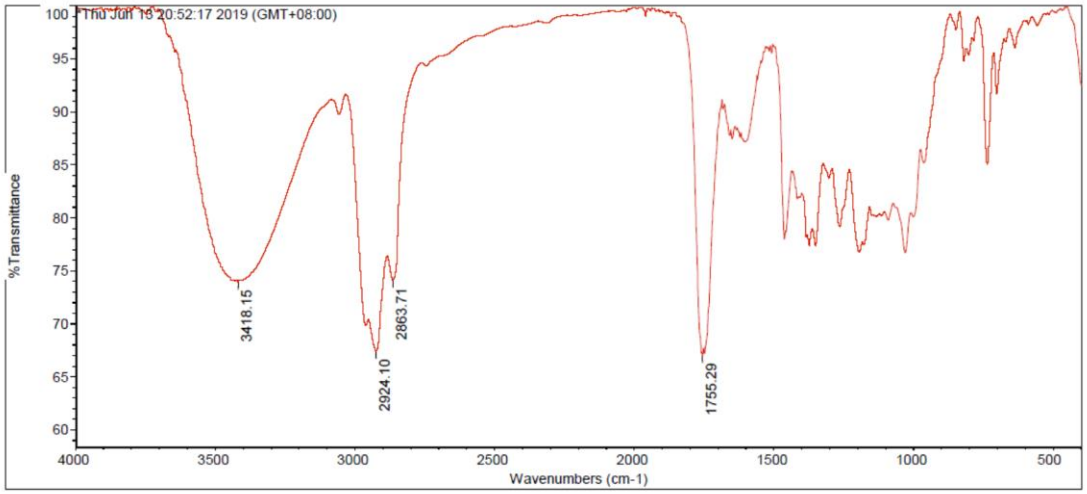

Thu Jun 13 20:55:26 2019 (GMT+08:00)
FIND PEAKS:
Spectrum: *Thu Jun 13 20:52:17 2019 (GMT+08:00)
Region: 4000.00 400.00
Absolute threshold: 74.949
Sensitivity: 50
Peak list:

Position:	1755.29	Intensity:	66.956
Position:	2863.71	Intensity:	74.130
Position:	2924.10	Intensity:	67.398
Position:	3418.15	Intensity:	73.954

Figure S31. IR spectrum of compound **3**

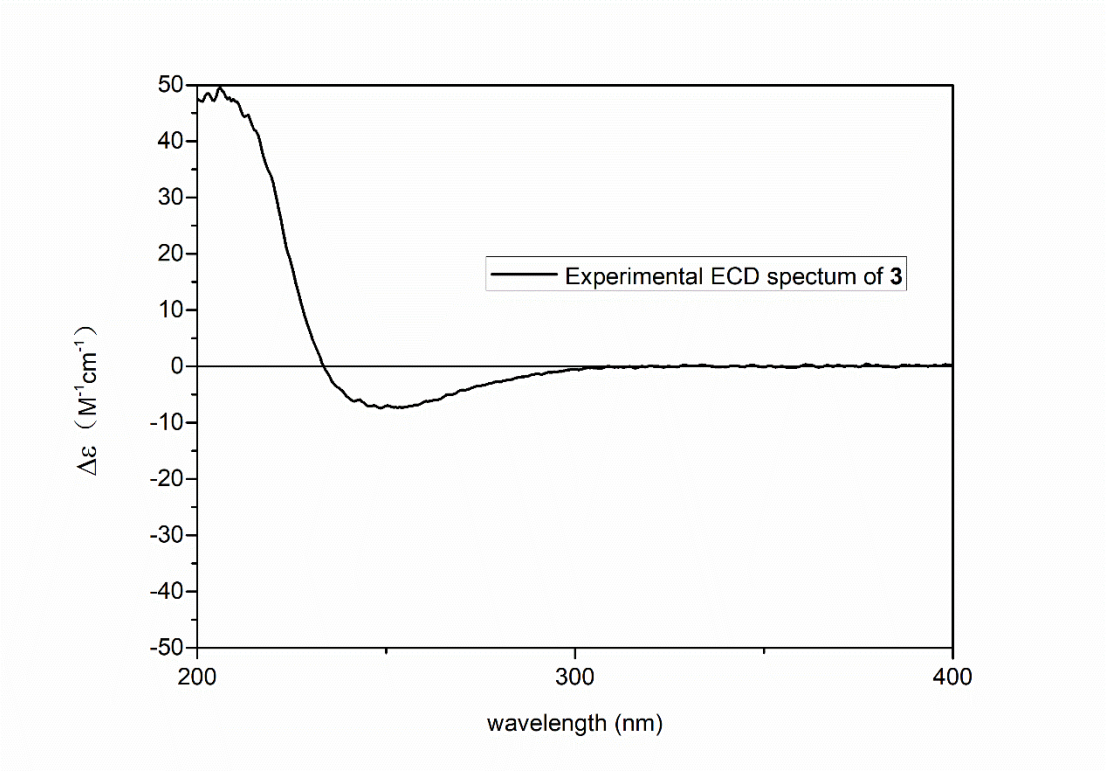

Figure S32. ECD spectrum of compound **3**

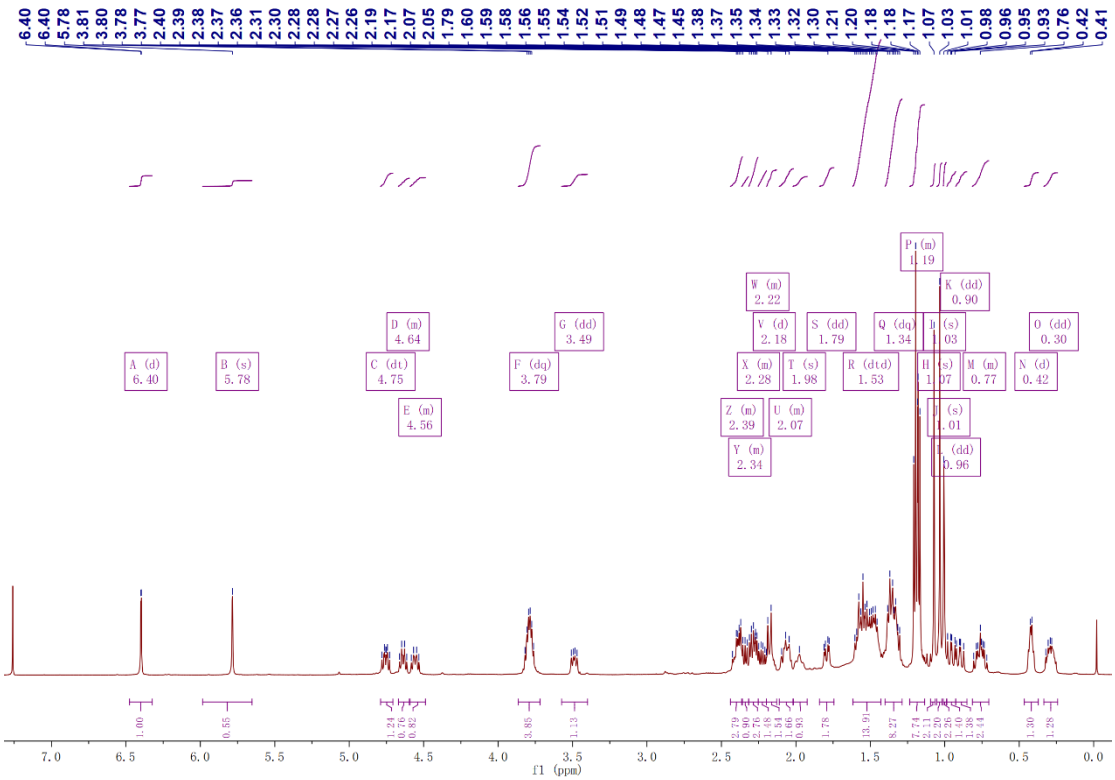

Figure S33. ^{1}H NMR spectrum of compound **3** in $CDCl_3$

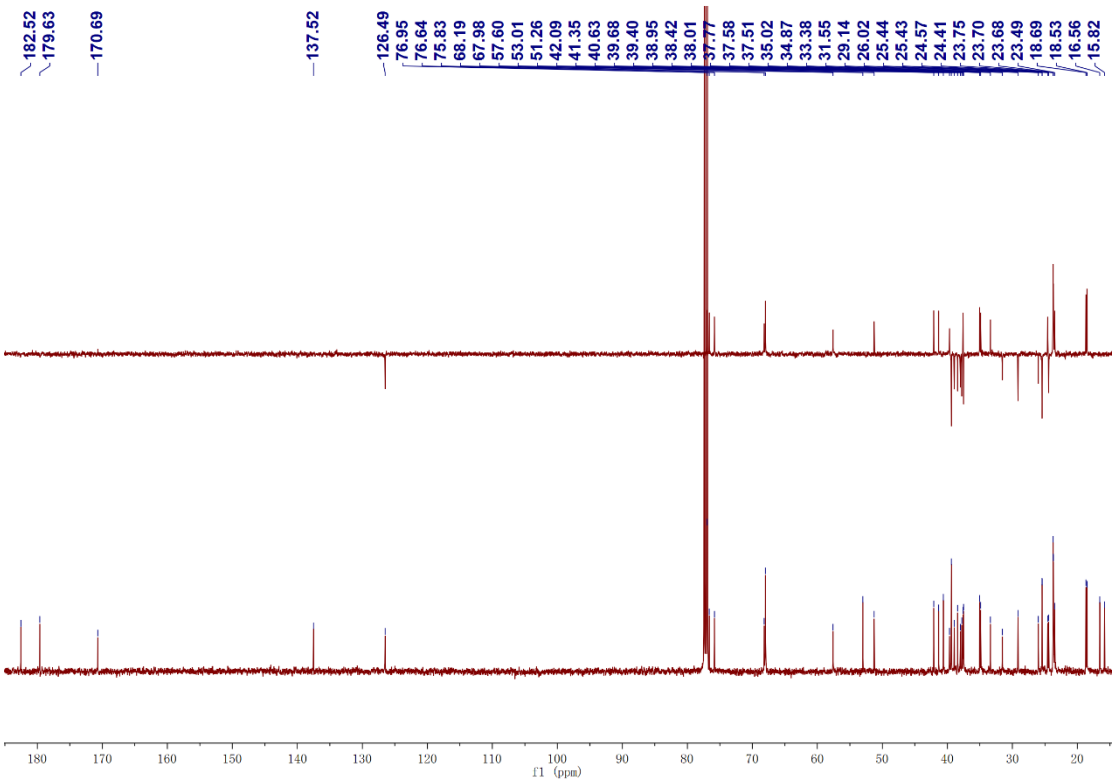

Figure S34. ^{13}C NMR spectrum of compound **3** in $CDCl_3$

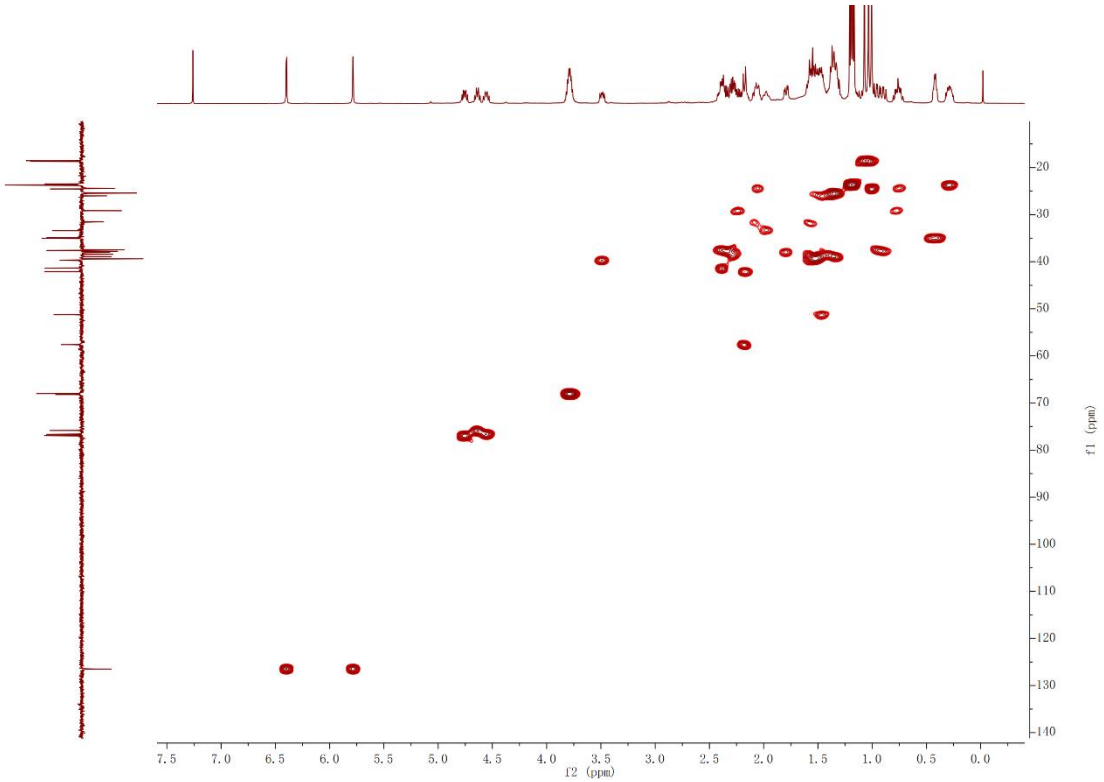

Figure S35. HSQC spectrum of compound **3** in $CDCl_3$

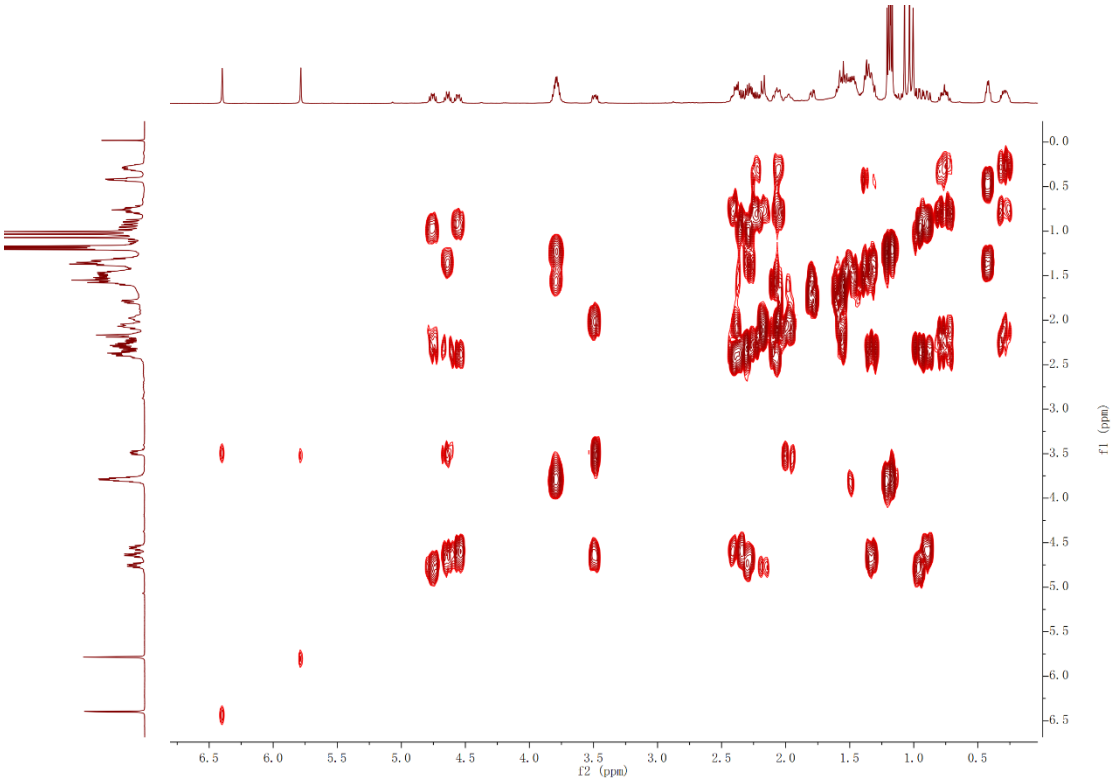

Figure S36. ^{1}H-^{1}H COSY spectrum of compound **3** in $CDCl_3$

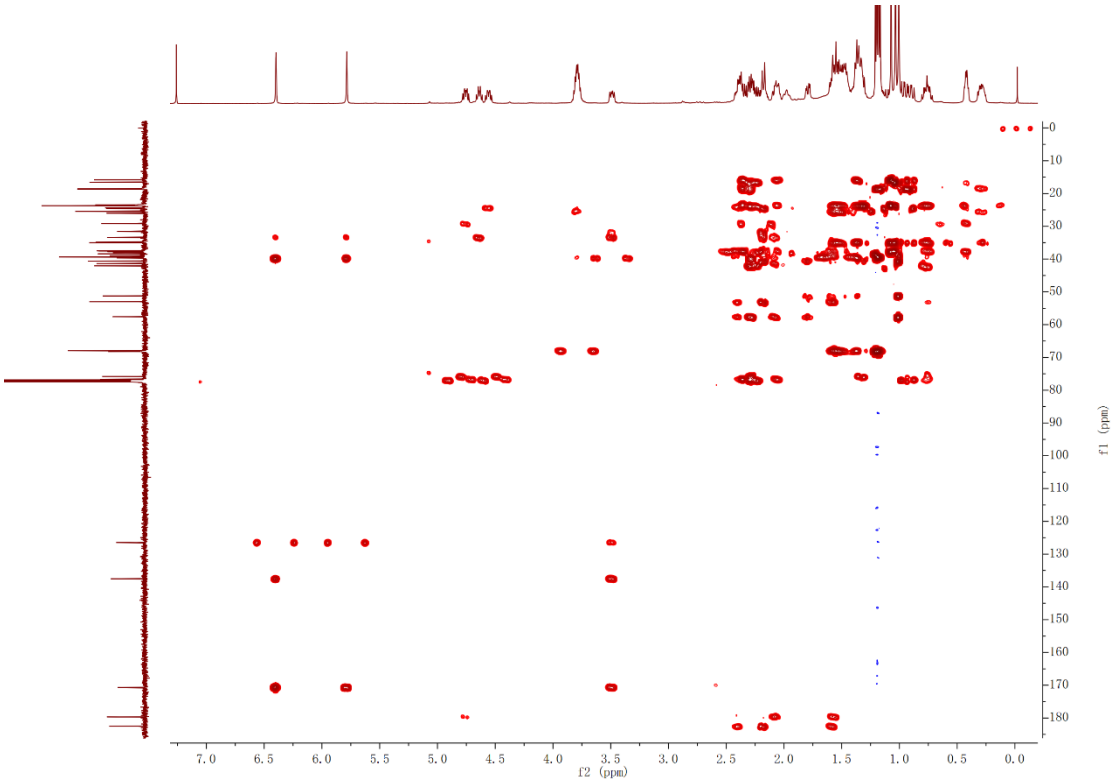

Figure S37. HMBC spectrum of compound **3** in $CDCl_3$

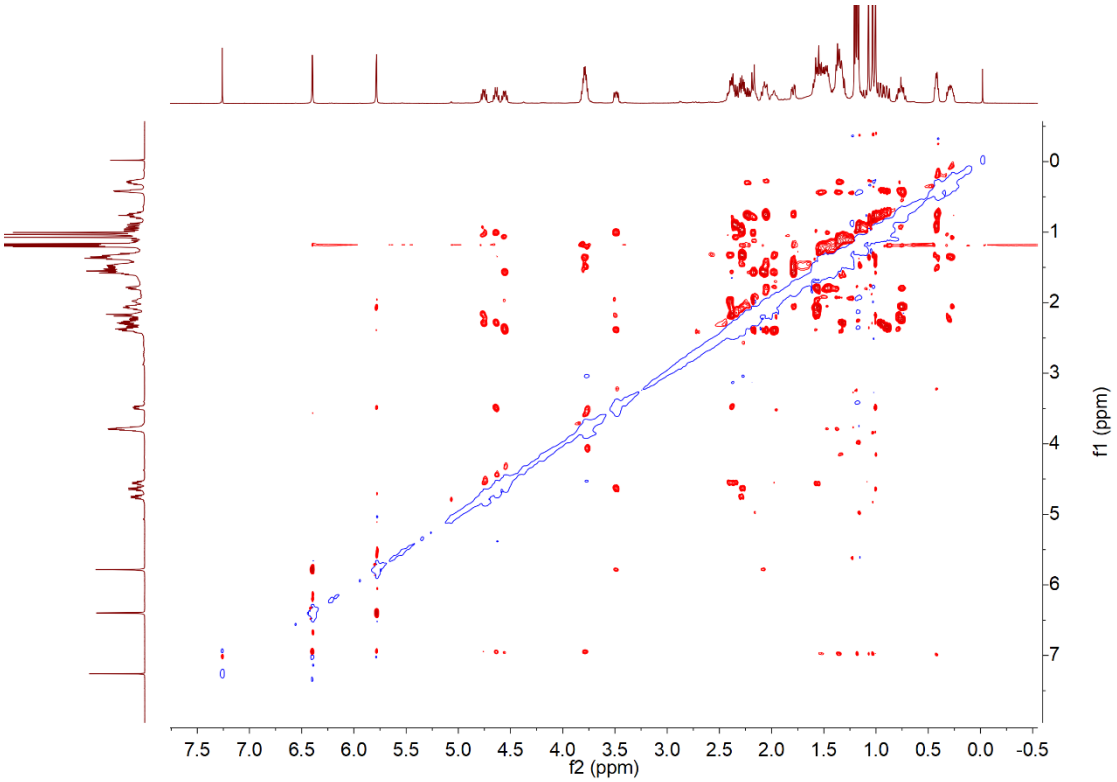

Figure S38. ROESY spectrum of compound **3** in $CDCl_3$

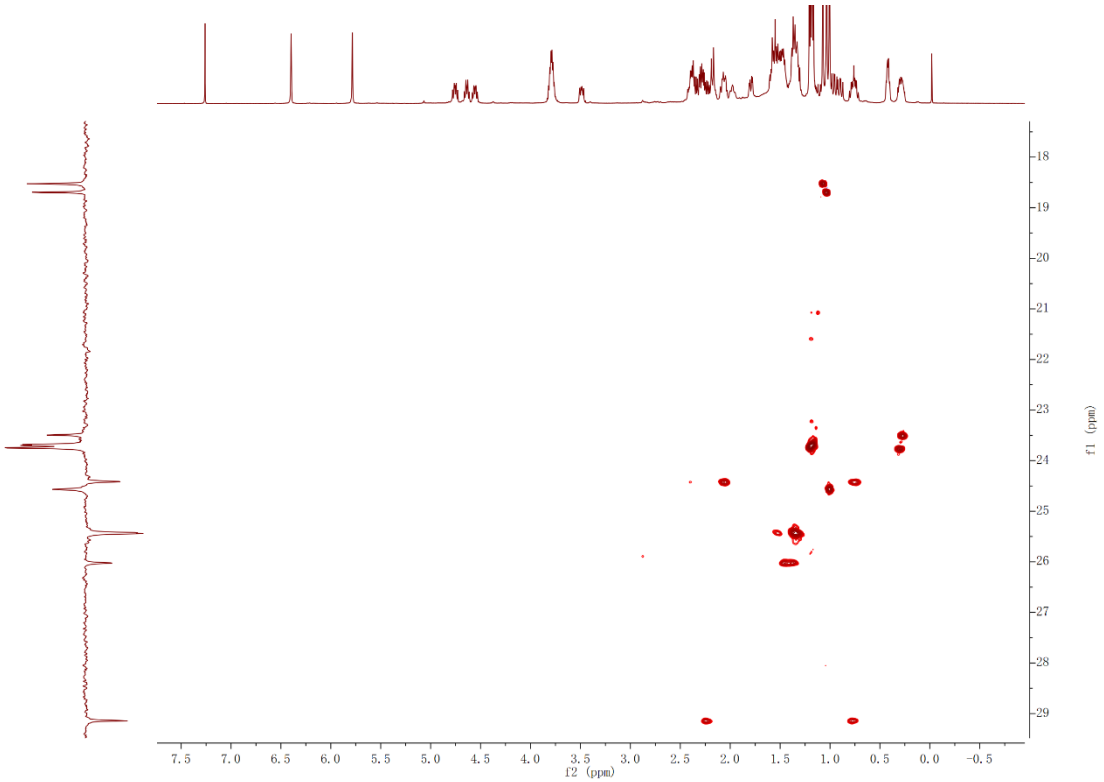

Figure S39. Selective HSQC (C15-30) spectrum of compound **3** in $CDCl_3$

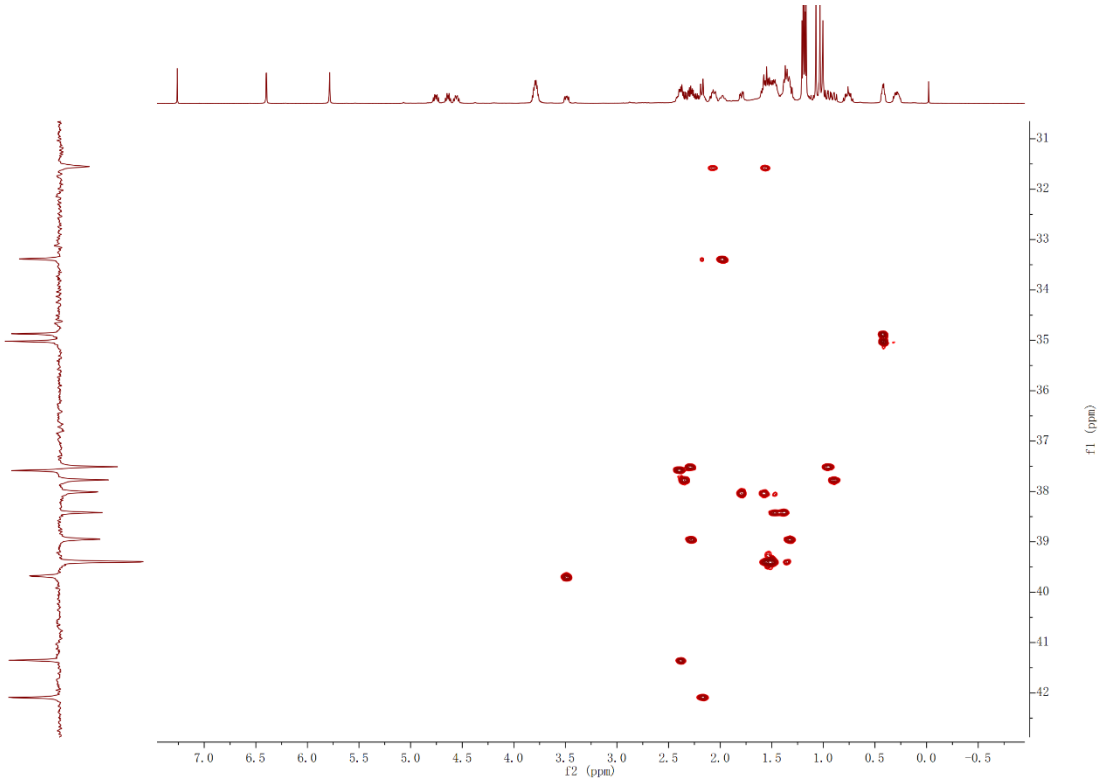

Figure S40. Selective HSQC (C30-45) spectrum of compound **3** in $CDCl_3$

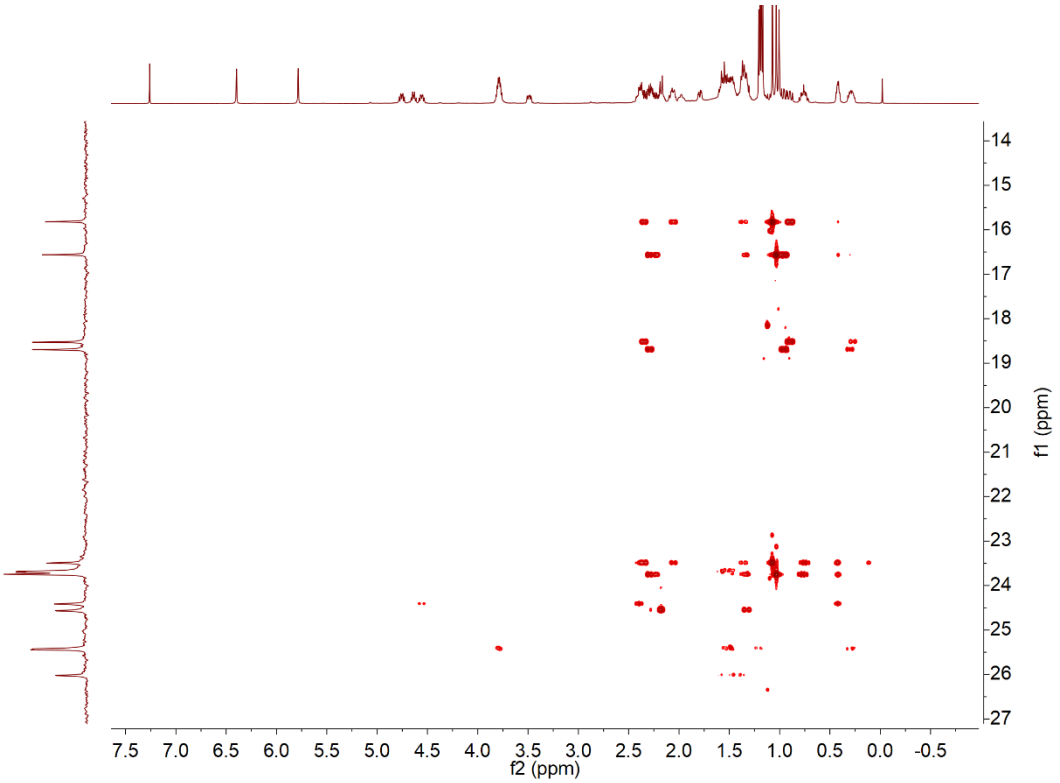

Figure S41. Selective HMBC (C15-30) spectrum of compound **3** in $CDCl_3$

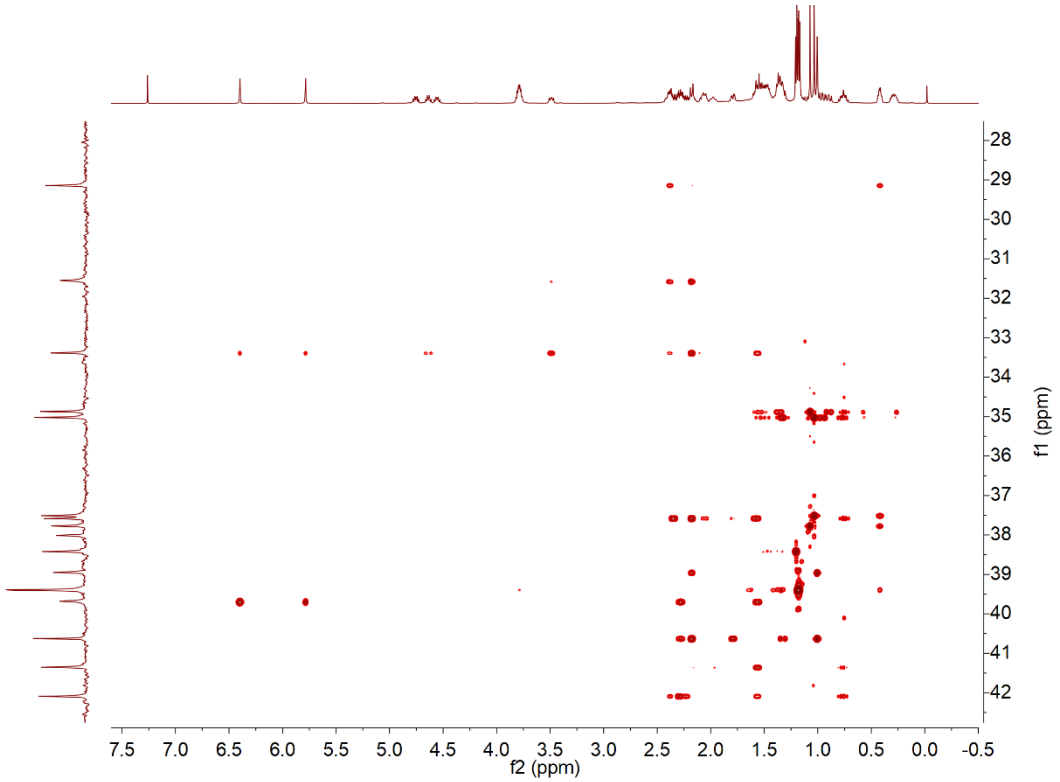

Figure S42. Selective HMBC (C28-45) spectrum of compound **3** in $CDCl_3$

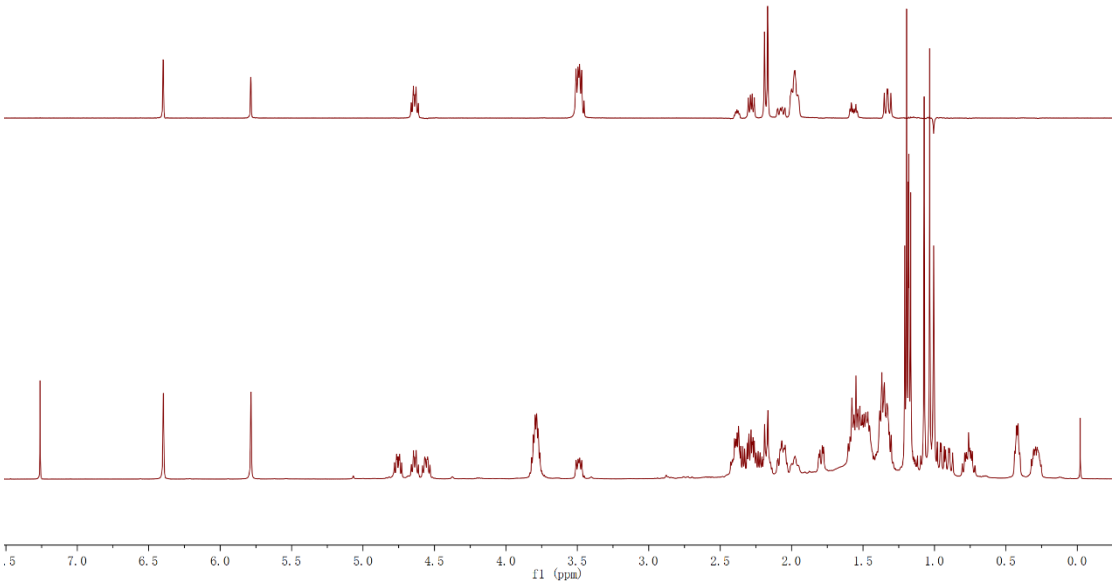

Figure S43. 1D-TOCSY (4.64 ppm) spectrum of compound **3** in $CDCl_3$

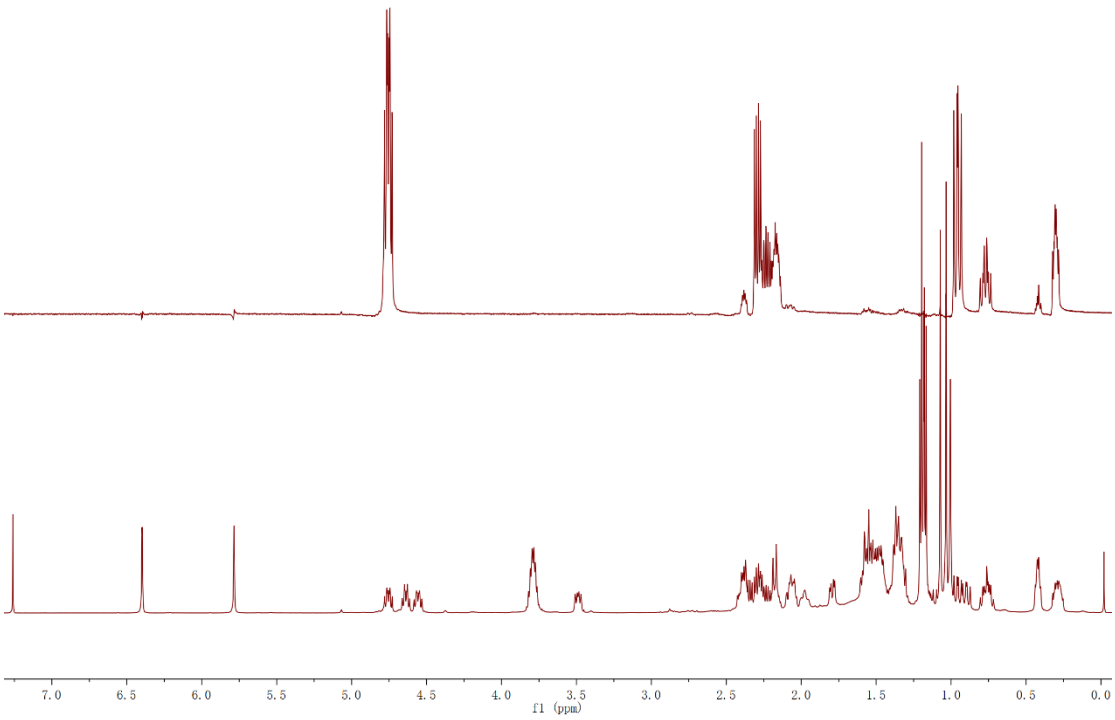

Figure S44. 1D-TOCSY (4.76 ppm) spectrum of compound **3** in $CDCl_3$

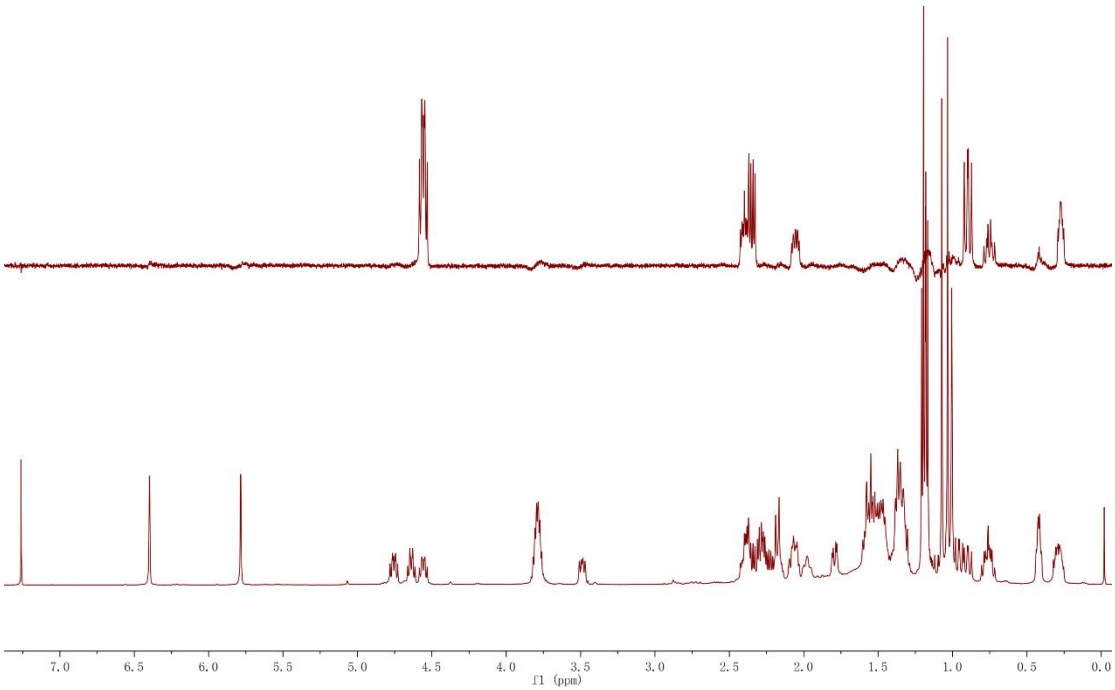

Figure S45. 1D-TOCSY (4.56 ppm) spectrum of compound **3** in $CDCl_3$

Table S1. Cytotoxicity of Compounds 1, 2, and 3 against CCRF-CEM and HCT-116 Cell Lines

Compound	IC50 (μM)	
	CCRF-CEM	HCT-116
1	>30	>30
2	>30	>30
3	25.36 ±4.07	>30
doxorubicin	0.08 ±0.02	0.78 ±0.05

The cytotoxicity of these three compounds against CCRF-CEM and HCT-116 cell lines was evaluated using the CCK-8 assay with doxorubicin as a positive control [m-20]. Unfortunately, only compound **3** exhibited cytotoxicity against CCRF-CEM cell with IC_{50} value of 25.4 μM, much weaker than that of the structurally related compounds dicarabrols A and B[m-19b] and faberidilactones A-E [m-12c]. Comparison of compounds **1-3** with the literature reported showed that the α-methylene-γ-lactone groups in **1-3** were destroyed or partially destroyed, which might account for the bioactivity decay. The results suggested that the α-methylene-γ-lactone group (αMγL) could be indispensable for cytotoxicity in this kind of structures as reported in literature [m-4].

Cytotoxicity Assays

The Cell Counting Kit 8 (CCK-8) assay was adopted to evaluate the cytotoxicity of the compounds against CCRF-CEM and HCT-116 cells. Cells seeded in 96-well plates were incubated in humidified air containing 5% CO_2 at 37 ℃ overnight. Appropriate dilutions of the test compounds were added to the cultures and incubated for another 72 h. At the end of the exposure time, 10 μL of CCK8

(Dojindo, Kumamoto, Japan) was added to each well and the plates were kept in the incubator for 4 h, then measured at 450 nm using a multiwell spectrophotometer (SpectraMax, Molecular Devices, USA). The cytotoxicity of compounds was expressed as an IC_{50}, determined by the Logit method. Doxorubicin was used as a positive control.

Computational details

The initial conformational search was performed by CONFLEX software[1,2] with the MMFF94s force field and an energy window of 3 kcal.mol^{-1} for choosing low-energy conformers. For compound 1, CONFLEX generated 4 conformers for 11′R*, and 9 conformers for 11′S*. For compound **3**, CONFLEX generated 7 conformers for 6′R*11″R*, 7 conformers for 6′R*11″S*, 12 conformers for 6′S*11″R*, and 8 conformers for 6′S*11″S*.

Then, DFT calculations were used for geometry optimization, Gibbs free energy, and NMR calculations of all conformers obtained from CONFLEX. All DFT calculations were performed using Gaussian 16 program.[3] An energy window of 3 kcal.mol^{-1} was used for DFT-optimized conformers. M062X[4]/6-31G(d)[5–7]/SMD[8](solvent=chloroform) were used for geometry optimizations and frequency calculations. Zero-point vibrational energies and thermal contributions to electronic energy were calculated at 298.15 K and 1 atm. All geometries were verified to be local minima without any imaginary frequencies. All vibrational frequencies below 50 cm^{-1} were replaced with values of 50 cm^{-1} due to the breakdown of the harmonic oscillator model for low frequency vibrational modes. To obtain better estimation of Gibbs free energies, single point electronic energies were computed using M062X/def2TZVP/SMD(solvent=chloroform). The resulting electronic energies were summed with the thermal free energy contributions computed at the M062X/6-31G(d)/SMD level to calculate to Boltzmann distribution. The gas constant R (0.001987204 kcal.K^{-1}.mol^{-1}) and room temperature (298.15 K) are used. Next, the theoretical predictions of ^{1}H and ^{13} C chemical shifts were calculated using mPW1PW91[9]/6-31G(d)/SMD(solvent=chloroform)/NMR(GIAO)[10] based on M062X/6-31G(d) optimized geometries. Final DFT-predicted chemical shifts were determined by scaling absolute computed isotropic values using scaling factors (slope=-1.0401, intercept=32.2587 for ^{1}H and slope=-0.9537, intercept=193.2179 for ^{13}C) obtained from http://cheshirenmr.info.[11] Finally, DP4+ analysis was utilized to determine the most probable configuration for each compound.[12]

Table S2. Calculated DFT free energies of four diastereoisomers (6′R*11″R*, 6′R*11″S*, 6′S*11″R*, and 6′S*11″S*) of compound **3** at M062X/def2TZVP/SMD(chloroform)//M062X/6-31G(d)/SMD(chloroform) level. Conformers with root-mean-square deviation of atomic positions (RMSD) smaller than 0.001 are considered as the same.

diastereoisomer	Conformers	DFT free energy (hartree)	Δ(DFT free energy) (kcal.mol^{-1})	%Population
6′R*11″R*	2	-1851.32461893	0.00	44.91%
	1	-1851.32405155	0.36	24.61%
	5	-1851.32349732	0.70	13.68%
	6	-1851.32309099	0.96	8.89%
	4	-1851.32290193	1.08	7.28%
	3	-1851.32059988	2.52	0.63%
6′R*11″S*	2	-1851.32009657	0.00	61.23%
	3	-1851.31945236	0.40	30.93%
	7	-1851.31752422	1.61	4.01%
	5	-1851.31687278	2.02	2.01%
	4	-1851.31677954	2.08	1.82%
6′S*11″R*	8	-1851.31651237	0.00	61.07%
	1	-1851.31522537	0.81	15.61%
	3	-1851.31477974	1.09	9.73%
	10	-1851.31457722	1.21	7.85%
	12	-1851.31401833	1.57	4.34%
	11	-1851.31236482	2.60	0.75%
	2	-1851.31222905	2.69	0.65%
6′S*11″S*	1	-1851.31178116	0.00	83.60%
	3	-1851.30940078	1.49	6.70%
	4	-1851.30927514	1.57	5.87%
	2	-1851.30867850	1.95	3.12%
	5	-1851.30728469	2.82	0.71%

3-6′R*11″R*-1	**3-6′R*11″R***-2	**3-6′R*11″R***-3	**3-6′R*11″R***-4
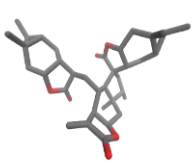	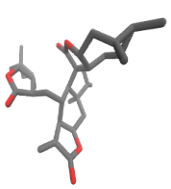	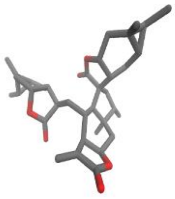	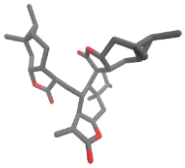

3-6′R*11″R*-5	**3-6′R*11″R* -6**	**3-6′R*11″S*-2**	**3-6′R*11″S*-3**
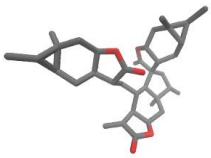	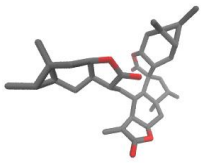	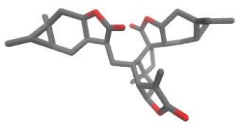	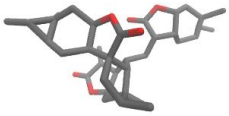
3-6′R*11″S*-4	**3-6′R*11″S*-5**	**3-6′R*11″S*-7**	**3-6′S*11″R*-1**
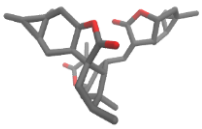	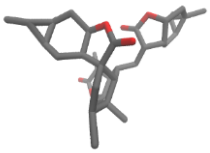	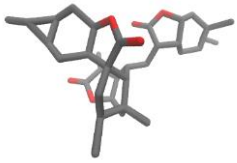	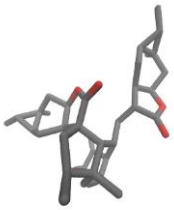
3-6′S*11″R*-2	**3-6′S*11″R*-3**	**3-6′S*11″R*-8**	**3-6′S*11″R*-10**
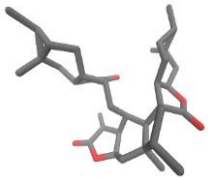	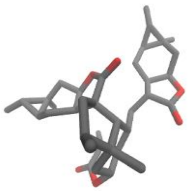	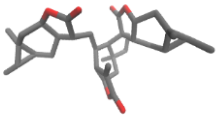	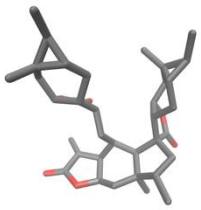
3-6′S*11″R*-11	**3-6′S*11″R*-12**	**3-6′S*11″S*-1**	**3-6′S*11″S*-2**
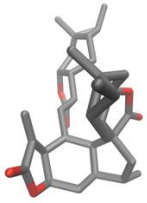	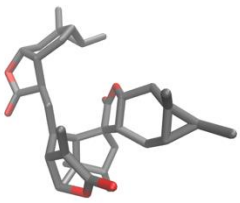	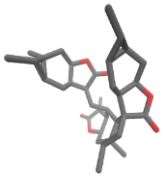	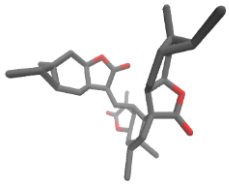
3-6′S*11″S*-3	**3-6′S*11″S*-4**	**3-6′S*11″S*-5**	
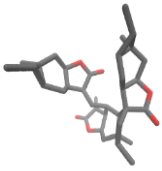	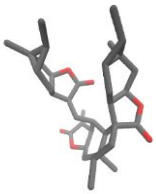	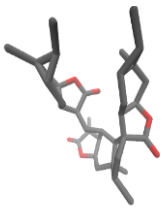	

Table S3. Comparison between computational and experimental ^{13}C chemical shifts for four diastereoisomers (6′R*11″R*, 6′R*11″S*, 6′S*11″R*, and 6′S*11″S*) of **3**. Computational results were obtained at mPW1PW91/6-31G(d)/SMD(chloroform)/ NMR(GIAO)//B3LYP/6-31G(d) level and scaled by δ_{scaled}= (193.2179 -δ_{calc})/0.9537.

Carbon	RR	RS	SR	SS	Exp.
1	29.20	28.74	28.93	28.48	**34.87**
5	24.97	24.19	24.37	25.60	**23.49**
6	25.38	26.18	26.51	27.07	**24.41**
7	40.49	42.31	39.92	41.88	**37.58**
8	77.08	77.67	75.93	76.17	**76.64**
9	37.84	37.07	36.76	37.71	**37.77**
10	16.63	16.98	17.22	17.32	**15.82**
11	54.86	57.00	53.18	55.31	**53.01**
12	182.83	184.42	183.65	184.47	**179.63**
13	40.15	40.42	43.92	40.59	**38.01**
14	18.45	18.18	18.03	18.25	**18.53**
1'	46.06	45.29	44.92	49.71	**51.26**
5'	58.23	59.35	59.07	63.00	**57.6**
6'	34.42	36.20	34.12	34.88	**33.38**
7'	41.99	44.22	41.05	45.95	**39.68**
8'	74.87	74.40	75.40	75.24	**75.83**
9'	38.57	41.07	43.11	41.15	**38.95**
10'	41.34	44.56	44.18	45.34	**40.63**
11'	139.71	143.20	139.78	141.38	**137.52**
12'	168.89	168.72	169.71	169.23	**170.69**
13'	129.62	127.68	128.31	128.01	**126.49**
14'	24.99	23.57	21.98	23.46	**24.57**
1''	29.60	29.35	30.60	29.61	**35.02**
5''	25.00	25.50	23.05	24.50	**23.74**
6''	28.98	23.98	32.44	25.26	**29.14**
7''	42.60	41.34	41.85	40.19	**41.35**
8''	77.24	76.43	76.68	75.96	**77.04**
9''	37.78	38.05	36.69	38.27	**37.51**
10''	17.62	16.24	19.26	16.47	**16.56**
11''	42.78	39.22	43.89	40.85	**42.09**
12''	180.71	180.19	179.05	179.00	**182.52**
13''	31.10	40.15	34.55	28.69	**31.55**
14''	18.62	19.38	18.07	19.03	**18.69**
RMSD	**2.1620**	**3.4375**	**2.7841**	**3.0150**	

Table S4. Comparison between computational and experimental ^{1}H chemical shifts for four diastereoisomers (6′R*11″R*,6′R*11″S*, 6′S*11″R*, and 6′S*11″S*) of 3. Computational results were obtained at mPW1PW91/6-31G(d)/SMD(chloroform)/ NMR(GIAO)//B3LYP/6-31G(d) level and scaled by δ_{scaled}= (32.2587 -δ_{calc})/1.0401.

Hydrogens	RR	RS	SR	SS	Exp.
1	0.69	0.62	0.66	0.62	**0.45**
5	0.48	0.37	0.36	0.32	**0.27**
6a	2.10	2.03	2.11	1.99	**2.06**
6b	0.88	0.84	0.97	0.87	**0.75**
7	2.61	2.23	2.70	2.39	**2.40**
8	4.58	4.83	4.77	4.84	**4.56**
9a	2.43	2.31	2.36	2.40	**2.35**
9b	0.97	0.80	0.97	0.86	**0.90**
13a	1.81	1.88	1.95	2.07	**1.79**
13b	1.67	1.67	1.55	1.87	**1.60**
14a	1.10	1.07	1.10	1.18	**1.07**
14b	1.10	1.07	1.10	1.18	**1.07**
14c	1.10	1.07	1.10	1.18	**1.07**
1'	1.93	1.92	1.90	2.03	**1.49**
5'	2.41	2.08	2.35	2.03	**2.18**
6'	2.22	3.16	3.10	3.97	**1.98**
7'	3.36	3.02	3.18	3.03	**3.49**
8'	4.47	4.67	4.60	4.66	**4.64**
9a'	2.33	2.06	2.05	2.46	**2.31**
9b'	1.55	1.39	1.41	1.69	**1.35**
13a'	6.47	6.70	6.53	6.39	**6.40**
13b'	6.12	6.49	6.28	5.99	**5.78**
14a'	1.06	1.13	1.16	1.18	**1.01**
14b'	1.06	1.13	1.16	1.18	**1.01**
14c'	1.06	1.13	1.16	1.18	**1.01**
1''	0.72	0.66	0.72	0.69	**0.44**
5''	0.51	0.46	0.46	0.47	**0.33**
6a''	2.05	1.92	2.33	2.08	**2.23**
6b''	1.00	0.80	1.21	0.94	**0.77**
7''	2.36	2.26	2.37	2.31	**2.41**
8''	4.75	4.68	4.57	4.52	**4.76**
9a''	2.43	2.58	2.17	2.49	**2.29**
9b''	0.97	1.00	1.08	1.01	**0.96**
11''	2.56	2.80	2.46	2.89	**2.19**
13a''	1.97	1.82	2.33	1.97	**2.07**
13b''	1.85	1.71	1.72	1.70	**1.56**
14a''	1.14	1.10	1.12	1.08	**1.03**
14b''	1.14	1.10	1.12	1.08	**1.03**
14c''	1.14	1.10	1.12	1.08	**1.03**
RMSD	**0.1743**	**0.2962**	**0.2663**	**0.3866**	

Table S5. DP4+ correlation for four diastereoisomers of **3** : 6′R*11″R* (Isomer 1), 6′R*11″S* (Isomer 2), 6′S*11″R* (Isomer 3), 6′S*11″S* (Isomer 4).

1	Functional	Solvent?		Basis Set		Type of Data	
2	mPW1PW91	PCM		6-31G(d)		Scaled Shifts	
3							
4		Isomer 1	Isomer 2	Isomer 3	Isomer 4	Isomer 5	Isomer 6
5	sDP4+ (H data)	100.00%	0.00%	0.00%	0.00%	-	-
6	sDP4+ (C data)	100.00%	0.00%	0.00%	0.00%	-	-
7	sDP4+ (all data)	100.00%	0.00%	0.00%	0.00%	-	-
8	uDP4+ (H data)	-	-	-	-	-	-
9	uDP4+ (C data)	-	-	-	-	-	-
10	uDP4+ (all data)	-	-	-	-	-	-
11	DP4+ (H data)	-	-	-	-	-	-
12	DP4+ (C data)	-	-	-	-	-	-
13	DP4+ (all data)	-	-	-	-	-	-

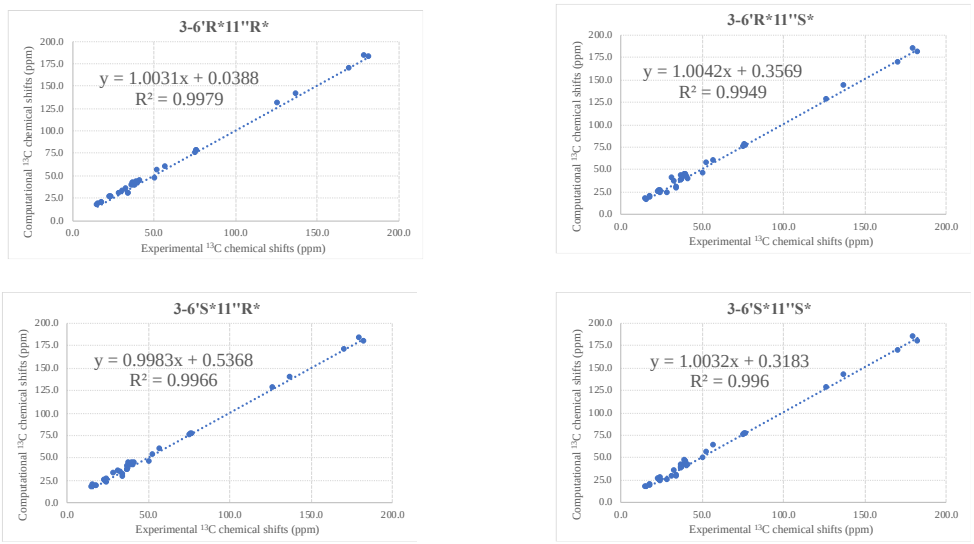

Figure S46. ^{13}C-NMR correlation for four diasteroisomers of **3**.

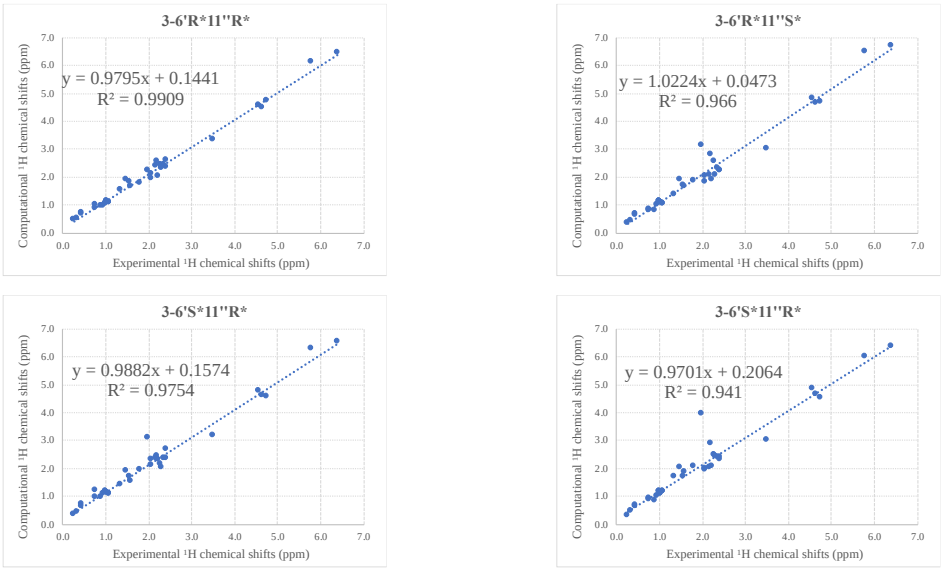

Figure S47. ^{1}H-NMR correlation for four diasteroisomers of **3**.

Table S6. Calculated DFT free energies of four diastereoisomers (11′R* and 11′S*) of **1** at M062X/def2TZVP/SMD(chloroform)//M062X/6-31G(d)/SMD(chloroform) level. Conformers with root-mean-square deviation of atomic positions (RMSD) smaller than 0.001 are considered as the same.

diastereoisomer	Conformers	DFT free energy (hartree)	Δ(DFT free energy) (kcal.mol^{-1})	%Population
11′R*	1	-1812.03927012	0.00	99.31%
	2	-1812.03458326	2.94	0.69%
11′S*	1	-1812.03571587	0.00	55.47%
	5	-1812.03492000	0.50	23.86%
	8	-1812.03386291	1.16	7.78%
	9	-1812.03364889	1.30	6.20%
	2	-1812.03342743	1.44	4.90%
	4	-1812.03247169	2.04	1.78%

1-11′R*-1	**1-11′R*-**2	**1-11′S*-**1	**1-11′S*-**2
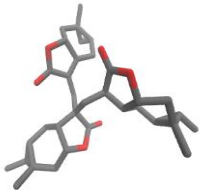	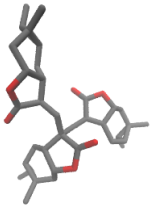	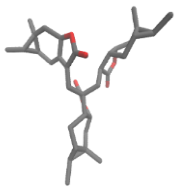	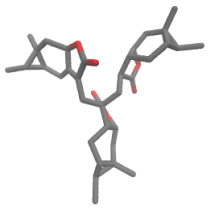
1-11′S*-4	**1-11′S*-5**	**1-11′S*-**8	**1-11′S*-**9
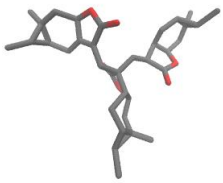	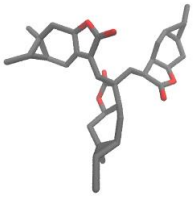	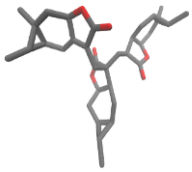	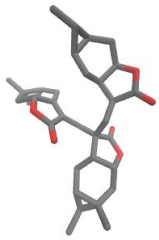

Table S7. Comparison between computational and experimental ^{13}C chemical shifts for two diastereoisomers (11′R* and 11′S*) of **1**. Computational results were obtained at mPW1PW91/6-31G(d)/SMD(chloroform)//NMR(GIAO)//B3LYP/6-31G(d) level and scaled by δ_{scaled}= (193.2179 -δ_{calc})/0.9537.

Carbons	1-11′R*	1-11′S*	Exp.
1	27.13	28.10	33.09
5	28.86	28.66	26.37
6	27.65	29.27	25.70
7	172.16	172.85	169.25
8	78.90	77.80	78.00
9	43.11	44.18	42.54
10	18.37	18.51	18.30
11	124.06	124.00	121.03
12	173.76	173.65	174.44
13	24.59	30.85	24.77
14	21.15	21.18	21.22
1'	29.55	28.52	35.10
5'	25.48	25.02	24.21
6'	29.00	23.54	29.20
7'	44.38	40.26	41.67
8'	77.07	76.95	76.99
9'	38.20	37.45	37.74
10'	16.78	16.28	16.30
11'	42.62	41.29	42.00
12'	180.30	180.05	179.02
13'	40.62	32.73	38.30
14'	18.89	19.46	18.95
1''	29.22	30.16	35.10
5''	25.27	24.95	24.21
6''	26.65	24.97	24.90
7''	47.80	46.97	44.94
8''	76.24	75.26	76.19
9''	38.49	37.86	38.10
10''	16.26	17.27	15.64
11''	48.42	47.91	47.29
12''	180.34	179.63	179.49
14''	18.87	18.95	19.03
RMSD	**2.2491**	**2.7896**	

Table S8. Comparison between computational and experimental ^{1}H chemical shifts for two diastereoisomers (11′R* and 11′S*) of **1**. Computational results were obtained at mPW1PW91/6-31G(d)/SMD(chloroform)/NMR(GIAO)//B3LYP/6-31G(d) level and scaled by $\delta_{scaled}= (32.2587 -\delta_{calc})/1.0401$.

Hydrogens	1-11′R*	1-11′S*	Exp.
1	0.49	0.42	0.14
5	0.83	0.79	0.66
6a	2.79	3.07	2.91
6b	2.97	2.86	2.84
8	5.05	4.76	4.89
9a	2.58	2.59	2.57
9b	1.43	1.30	1.35
13a	2.86	2.43	2.74
13b	2.24	2.36	2.32
14a	1.18	1.17	1.14
14b	1.18	1.17	1.14
14c	1.18	1.17	1.14
1'	0.63	0.63	0.40
5'	0.50	0.51	0.30
6′a	2.27	2.08	2.26
6′b	0.73	0.70	0.66
7'	1.94	2.24	1.99
8'	4.64	4.48	4.70
9′a	2.44	2.46	2.32
9′b	0.87	0.96	0.93
11'	2.10	2.62	2.02
13′a	2.02	2.43	1.94
13′b	1.67	1.75	1.89
14a	1.05	1.07	1.02
14b	1.05	1.07	1.02
14c	1.05	1.07	1.02
1''	0.66	0.70	0.43
5''	0.68	0.53	0.43
6''a	2.89	2.30	2.61
6''b	0.69	1.00	0.64
7''	2.49	2.50	2.53
8''	4.84	4.81	4.89
9''a	2.53	2.48	2.46
9''b	0.93	1.14	0.99
14a	1.13	1.14	1.06
14b	1.13	1.14	1.06
14c	1.13	1.14	1.06
RMSD	**0.1324**	**0.2010**	

Table S9. DP4+ correlation for two diastereoisomers of **1** : 11′R* (Isomer 1), and 11′S* (Isomer 2).

Functional	Solvent?	Basis Set	Type of Data			
mPW1PW91	PCM	6-31G(d)	Scaled Shifts			
	Isomer 1	Isomer 2	Isomer 3	Isomer 4	Isomer 5	Isomer 6
sDP4+ (H data)	100.00%	0.00%	-	-	-	-
sDP4+ (C data)	99.99%	0.01%	-	-	-	-
sDP4+ (all data)	100.00%	0.00%	-	-	-	-
uDP4+ (H data)	-	-	-	-	-	-
uDP4+ (C data)	-	-	-	-	-	-
uDP4+ (all data)	-	-	-	-	-	-
DP4+ (H data)	-	-	-	-	-	-
DP4+ (C data)	-	-	-	-	-	-
DP4+ (all data)	-	-	-	-	-	-

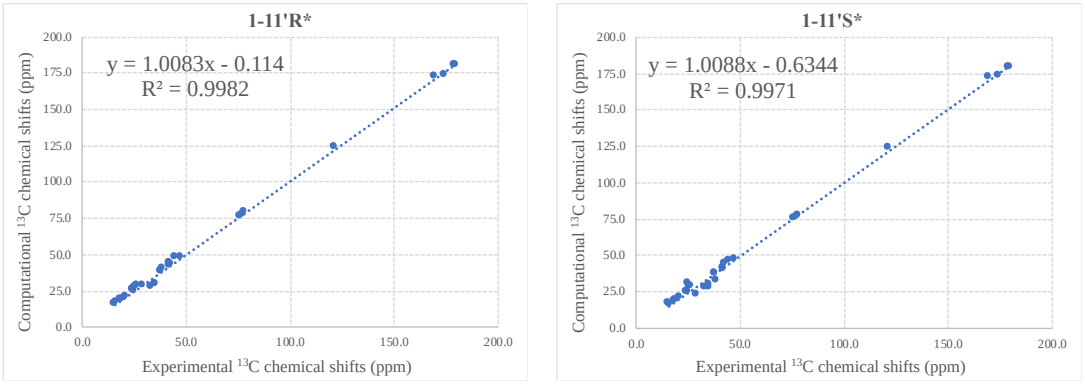

Figure S48. ^{13}C-NMR correlation for two diastereoisomers of **1**.

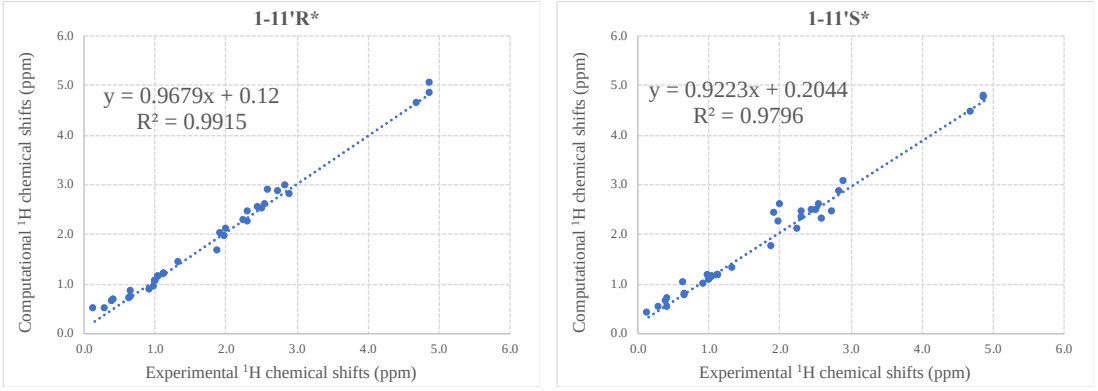

Figure S49. ^{1}H-NMR correlation for two diastereoisomers of **1**.

References

(1) Goto, H.; Osawa, E. Corner Flapping: A Simple and Fast Algorithm for Exhaustive Generation of Ring Conformations. *J. Am. Chem. Soc.* **1989**, *111* (24), 8950–8951. https://doi.org/10.1021/ja00206a046.

(2) Gotō, H.; Ōsawa, E. An Efficient Algorithm for Searching Low-Energy Conformers of Cyclic and Acyclic Molecules. *J. Chem. Soc., Perkin Trans. 2* **1993**, No. 2, 187–198. https://doi.org/10.1039/P29930000187.

(3) Gaussian 16, Revision B.01, M. J. Frisch, G. W. Trucks, H. B. Schlegel, G. E. Scuseria, M. A. Robb, J. R. Cheeseman, G. Scalmani, V. Barone, G. A. Petersson, H. Nakatsuji, X. Li, M. Caricato, A. V. Marenich, J. Bloino, B. G. Janesko, R. Gomperts, B. Mennucci, H. P. Hratchian, J. V. Ortiz, A. F. Izmaylov, J. L. Sonnenberg, D. Williams-Young, F. Ding, F. Lipparini, F. Egidi, J. Goings, B. Peng, A. Petrone, T. Henderson, D. Ranasinghe, V. G. Zakrzewski, J. Gao, N. Rega, G. Zheng, W. Liang, M. Hada, M. Ehara, K. Toyota, R. Fukuda, J. Hasegawa, M. Ishida, T. Nakajima, Y. Honda, O. Kitao, H. Nakai, T. Vreven, K. Throssell, J. A. Montgomery, Jr., J. E. Peralta, F. Ogliaro, M. J. Bearpark, J. J. Heyd, E. N. Brothers, K. N. Kudin, V. N. Staroverov, T. A. Keith, R. Kobayashi, J. Normand, K. Raghavachari, A. P. Rendell, J. C. Burant, S. S. Iyengar, J. Tomasi, M. Cossi, J. M. Millam, M. Klene, C. Adamo, R. Cammi, J. W. Ochterski, R. L. Martin, K. Morokuma, O. Farkas, J. B. Foresman, and D. J. Fox, Gaussian, Inc., Wallingford CT, 2016.

(4) Zhao, Y.; Truhlar, D. G. The M06 Suite of Density Functionals for Main Group Thermochemistry, Thermochemical Kinetics, Noncovalent Interactions, Excited States, and Transition Elements: Two New Functionals and Systematic Testing of Four M06-Class Functionals and 12 Other Function. *Theor. Chem. Acc.* **2008**, *120* (1), 215–241. https://doi.org/10.1007/s00214-007-0310-x.

(5) Ditchfield, R.; Hehre, W. J.; Pople, J. A. Self-Consistent Molecular-Orbital Methods. IX. An Extended Gaussian-Type Basis for Molecular-Orbital Studies of Organic Molecules. *J. Chem. Phys.* **1971**, *54* (2), 724–728. https://doi.org/10.1063/1.1674902.

(6) Hehre, W. J.; Ditchfield, R.; Pople, J. A. Self—Consistent Molecular Orbital Methods. XII. Further Extensions of Gaussian—Type Basis Sets for Use in Molecular Orbital Studies of Organic Molecules. *J. Chem. Phys.* **1972**, *56* (5), 2257–2261. https://doi.org/10.1063/1.1677527.

(7) Hariharan, P. C.; Pople, J. A. The Influence of Polarization Functions on Molecular Orbital Hydrogenation Energies. *Theor. Chim. Acta* **1973**, *28* (3), 213–222. https://doi.org/10.1007/BF00533485.

(8) Marenich, A. V.; Cramer, C. J.; Truhlar, D. G. Universal Solvation Model Based on Solute Electron Density and on a Continuum Model of the Solvent Defined by the Bulk Dielectric Constant and Atomic Surface Tensions. *J. Phys. Chem. B* **2009**, *113* (18), 6378–6396. https://doi.org/10.1021/jp810292n.

(9) Adamo, C.; Barone, V. Exchange Functionals with Improved Long-Range Behavior and Adiabatic Connection Methods without Adjustable Parameters: The MPW and MPW1PW Models. *J. Chem. Phys.* **1998**, *108* (2), 664–675. https://doi.org/10.1063/1.475428.

(10) Wolinski, K.; Hinton, J. F.; Pulay, P. Efficient Implementation of the Gauge-Independent Atomic Orbital Method for NMR Chemical Shift Calculations. *J. Am. Chem. Soc.* **1990**, *112* (23), 8251–8260. https://doi.org/10.1021/ja00179a005.

(11) CHESHIRE Chemical Shift Repository http://cheshirenmr.info/index.htm (accessed Oct 29,

2019).

(12) Grimblat, N.; Zanardi, M. M.; Sarotti, A. M. Beyond DP4: An Improved Probability for the Stereochemical Assignment of Isomeric Compounds Using Quantum Chemical Calculations of NMR Shifts. *J. Org. Chem.* **2015**, *80* (24), 12526–12534. https://doi.org/10.1021/acs.joc.5b02396.